

Fragment-Based Approach to Targeting Inosine-5'-monophosphate Dehydrogenase (IMPDH) from *Mycobacterium tuberculosis*

Ana Trapero,[†] Angela Pacitto,[‡] Vinayak Singh,^{§,#} Mohamad Sabbah,[†] Anthony G. Coyne,[†] Valerie Mizrahi,[§] Tom L. Blundell,^{*,‡} David B. Ascher,^{*,‡,||} and Chris Abell^{*,†}

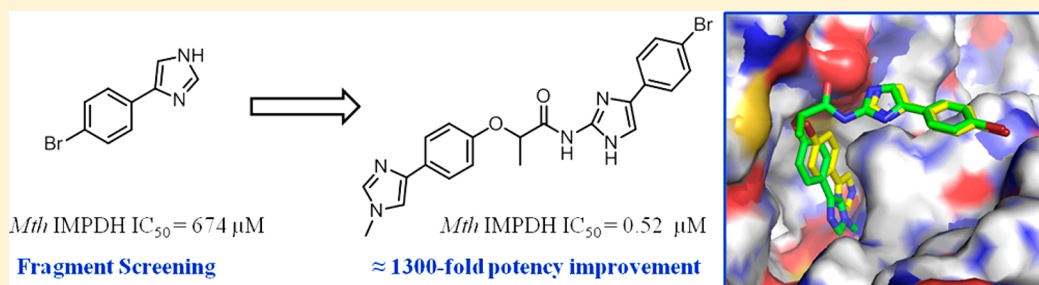
[†]Department of Chemistry, University of Cambridge, Lensfield Road, Cambridge CB2 1EW, United Kingdom

[‡]Department of Biochemistry, University of Cambridge, 80 Tennis Court Road, Cambridge CB2 1GA, United Kingdom

[§]MRC/NHLS/UCT Molecular Mycobacteriology Research Unit & DST/NRF Centre of Excellence for Biomedical TB Research, Institute of Infectious Disease and Molecular Medicine and Division of Medical Microbiology, Faculty of Health Sciences, University of Cape Town, Rondebosch 7701, Cape Town, South Africa

^{||}Department of Biochemistry and Molecular Biology, Bio21 Institute, University of Melbourne, 30 Flemington Road, Parkville, Victoria 3052, Australia

S Supporting Information



ABSTRACT: Tuberculosis (TB) remains a major cause of mortality worldwide, and improved treatments are needed to combat emergence of drug resistance. Inosine 5'-monophosphate dehydrogenase (IMPDH), a crucial enzyme required for *de novo* synthesis of guanine nucleotides, is an attractive TB drug target. Herein, we describe the identification of potent IMPDH inhibitors using fragment-based screening and structure-based design techniques. Screening of a fragment library for *Mycobacterium thermoresistibile* (*Mth*) IMPDH ΔCBS inhibitors identified a low affinity phenylimidazole derivative. X-ray crystallography of the *Mth* IMPDH ΔCBS–IMP–inhibitor complex revealed that two molecules of the fragment were bound in the NAD binding pocket of IMPDH. Linking the two molecules of the fragment afforded compounds with more than 1000-fold improvement in IMPDH affinity over the initial fragment hit.

■ INTRODUCTION

Tuberculosis (TB) is a contagious infectious disease caused by *Mycobacterium tuberculosis* (*Mtb*), which can be transmitted through the air as droplets. The infection predominantly affects the lungs, but it can spread to other parts of the body, especially in patients with a suppressed immune system.

The World Health Organization (WHO) has estimated that nearly one-third of the world's population is infected with *Mtb*, leading to 1.8 million TB deaths in 2015.¹ Although there has been a slow decline in new TB cases and TB-related deaths in recent years, the emergence and spread of multidrug resistant (MDR) and extensively drug resistant (XDR) strains of *Mtb* has increased the threat that this disease poses for global public health. According to the WHO, approximately 480,000 cases of MDR-TB emerged in 2015, and the cure rate of those patients was only 50%.¹

Current TB treatments require combinations of four first-line drugs, isoniazid, rifampicin, ethambutol, pyrazinamide, and streptomycin, which must be taken for six months or longer.²

Resistant strains are not susceptible to the standard drugs, and although MDR-TB is treatable using second-line drugs, such treatments have a number severe side effects.³ Consequently, there is an urgent need for the development of novel and more effective drugs for the treatment of drug resistant TB.

Inosine-5'-monophosphate dehydrogenase (IMPDH, E.C. 1.1.1.205) has received considerable interest in recent years as an important target enzyme for immunosuppressive,⁴ anti-cancer,^{5,6} and antiviral drugs.⁷ Most recently, IMPDH has emerged as a promising antimicrobial drug target.^{8–11}

IMPDH catalyzes the first unique step in the *de novo* synthesis of guanine nucleotides, the oxidation of inosine 5'-monophosphate (IMP) to xanthosine 5'-monophosphate (XMP) with the concomitant reduction of the cofactor nicotinamide adenine dinucleotide (NAD⁺) to NADH (Figure 1).¹² XMP is then

Received: November 2, 2017

Published: March 16, 2018

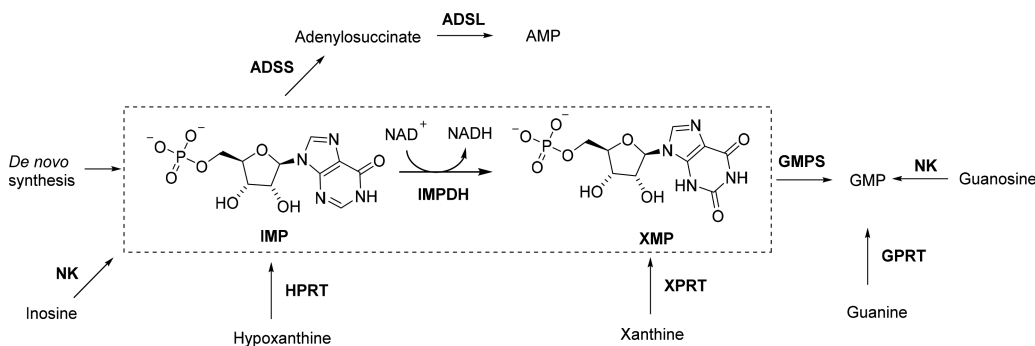


Figure 1. Purine nucleotide biosynthesis. The commonly occurring guanine nucleotide biosynthetic and salvage reactions are shown, as is the adenine nucleotide biosynthetic pathway. The IMPDH reaction is boxed. NK, nucleoside kinase; HPRT, hypoxanthine phosphoribosyl transferase; XPRTP, xanthine phosphoribosyl transferase; GPRT, guanine phosphoribosyl transferase; GMPS, guanosine 5'-monophosphate synthetase; GMPR, guanosine 5'-monophosphate reductase; ADSS, adenylosuccinate synthetase; ADSL, adenylosuccinate lyase.

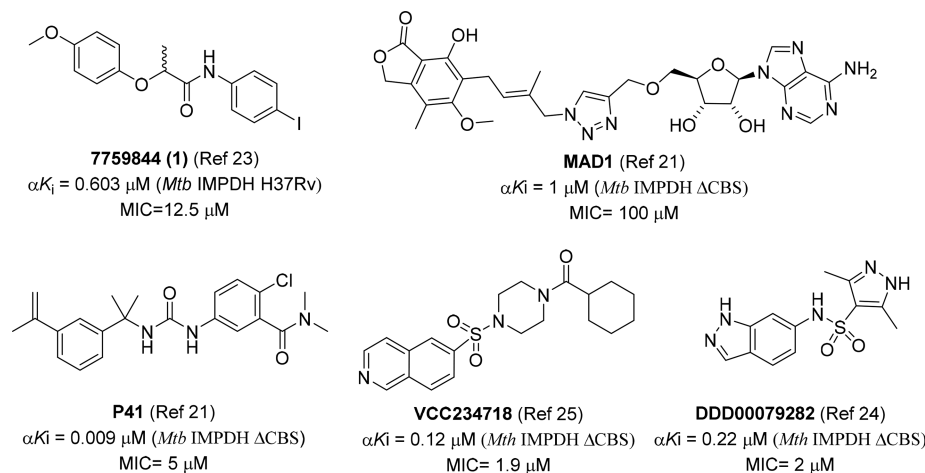


Figure 2. Structures of previously reported IMPDH inhibitors (αK_i values against IMP). All compounds showed uncompetitive inhibition with respect to IMP.

subsequently converted to guanosine 5'-monophosphate (GMP) by a GMP synthetase.¹⁵

IMPDH has been deemed essential in every pathogen analyzed to date, including *Mtb*, *Staphylococcus aureus*, and *Pseudomonas aeruginosa*, which are three of the most serious bacterial threats.^{14–16} However, this has been somewhat contradictory,¹⁷ in comparing cell versus animal work. IMPDH is an ubiquitous enzyme present in several eukaryotes, bacteria, and protozoa.¹⁸ The IMPDH reaction involves two chemical transformations. The first step of the IMPDH catalyzed reaction involves the attack of catalytic Cys on substrate IMP followed by hydride transfer to NAD^+ , forming the covalent enzyme intermediate E-XMP*. In the second step, E-XMP* is hydrolyzed to XMP.¹¹ The enzyme exists in two different conformations, an open form that accommodates both the substrate and cofactor during the first step and a closed form where the active site flap moves into the NAD^+ -binding site for the E-XMP* hydrolysis.¹⁹

In recent years, there has been considerable effort aimed at identifying small molecule inhibitors of IMPDH as potential antitubercular agents. X-ray crystal structures of a truncated form of the *Mtb* enzyme in complex with some of these compounds have been reported.^{20–26}

In antibacterial drug discovery, and especially in TB drug discovery, high-throughput screening (HTS) typically identifies a number of leads that show high potency *in vitro*, but most did

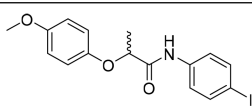
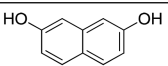
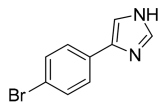
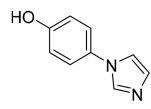
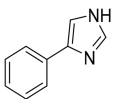
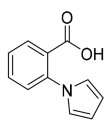
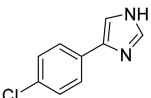
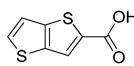
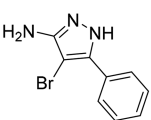
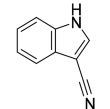
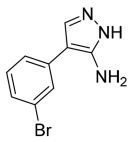
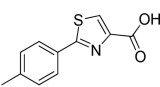
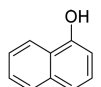
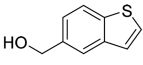
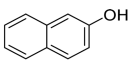
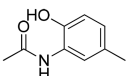
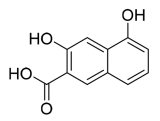
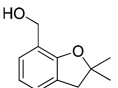
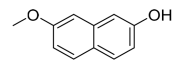
not show any translation to an *in vivo* effect. It is also inevitable that the HTS libraries represent only a small fraction of possible chemical space and so limit confidence in finding a good starting point for subsequent development. Phenotypic screens can potentially lead to the identification of a molecule that modifies a disease phenotype by acting on a previously undescribed target or by acting simultaneously on more than one target.²⁷ However, for many of these hits the relevant target or targets has not yet been identified, thus preventing further target-based optimization of the compounds.^{28,29}

The previously reported IMPDH inhibitors, such as compounds 7759844 (1), MAD1, P41, VCC234718, and DDD00079282 (Figure 2), were identified by phenotypic screening or target based HTS of compound libraries.^{21,23–25}

We have sought to develop IMPDH inhibitors using a fragment-based approach. Fragment-based drug discovery (FBDD) is now established in both industry and academia as an alternative approach to high-throughput screening for the generation of hits or chemical tools for drug targets.³⁰

We have previously reported the discovery of several series of novel and potent inhibitors using FBDD to target *Mtb*. Previously we have reported the fragment elaboration strategies that we have applied which have included fragment growing, merging, and linking. Although fragment linking is conceptually the most appealing strategy for fragment elaboration, in practice,

Table 1. Structures and Activities for Compound 1 (7759844) and the Most Potent Fragment Hits Found in the Screen against *Mth* IMPDH Δ CBS

Compd	Structure	% Inhibition at 1 mM	Compd	Structure	% Inhibition at 1 mM
1		92 ± 1 ^a	11		77 ± 1
2		65 ± 2	12		64 ± 6
3		52 ± 4	13		72 ± 1
4		59 ± 1	14		86 ± 6
5		53 ± 3	15		51 ± 1
6		50 ± 3	16		88 ± 10
7		68 ± 3	17		53 ± 2
8		57 ± 1	18		79 ± 4
9		98 ± 2	19		99 ± 1
10		66 ± 1			

^a% Inhibition at 10 μ M.

this strategy can be challenging where the choice of the optimal fragment linker can be crucial.^{31,32}

In the fragment-based approach, biophysical techniques are usually used to identify small chemical compounds (fragments) that bind with low affinity to the drug target. X-ray crystallography is then usually employed to establish the binding mode of the fragment and to facilitate the design of elaborated fragments. The availability of high-resolution X-ray crystal structures of a truncated form of the IMPDH,^{21,24,25} in both the substrate-free and substrate/ligand-bound forms, makes this enzyme attractive for a fragment-based approach.

In this work, the discovery of a new class of potent nM inhibitors of IMPDH using a FBDD approach is reported. A library of 960 fragments was screened against *Mth* IMPDH Δ CBS using a biochemical assay. The fragment hits from this assay were examined using X-ray crystallography, and an X-ray crystal structure of one of the fragment complexes was solved to a

resolution of 1.45 Å. Examination of the X-ray crystal structure suggested a strategy of fragment-linking for optimization of this fragment hit.

RESULTS AND DISCUSSION

Fragment Screening. An in-house fragment library composed of 960 fragments was screened using a biochemical assay against *Mth* IMPDH Δ CBS. *Mth* IMPDH, which shares 85% sequence identity with *Mtb* IMPDH and is 100% identical in the active site,^{24,25} was chosen for the fragment screening and structural studies because it gave higher protein expression yields and better diffracting crystals than the *Mtb* orthologue. IMPDH activity was monitored spectrophotometrically by measuring the formation of NADH at 340 nm. The biochemical assay was performed at a fragment concentration of 1 mM, and hits were retested in triplicate. Compound 1 (7759844) previously

reported as IMPDH inhibitor was used as a positive control in assays (Table 1).²³

The screen resulted in 18 hits (1.9% hit rate), where a hit was defined as a compound that gave greater than 50% inhibition at a concentration of 1 mM. A complete list of fragment hits identified is included in Table 1. A number of common scaffolds were observed, in particular phenylimidazole (fragments 2–4), aminopyrazole (fragments 5–6), and naphthol (fragments 7–11), and the remaining compounds contained a substituted phenyl or a heterocyclic five membered ring (fragments 12–19).

The IC₅₀ values of six of the most active fragments were measured and the IC₅₀ and ligand efficiency (LE) values of these fragments are summarized in Table 2. The fragment screen

Table 2. IC₅₀, Ligand Efficiency, and Alpha K_i Values of Fragment Hits and Compound 1 (7759844) against *Mth* IMPDH ΔCBS

Compd	IC ₅₀ (μM) (LE) ^a	IMP αK _i (μM)	NAD αK _i (μM)
1	0.77 ± 0.06 (0.40)	0.86 ± 0.03 (UC) ^b	0.55 ± 0.02 (UC)
2	674 ± 53 (0.36)	609 ± 3 (UC)	512 ± 23 (UC)
11	336 ± 6 (0.39)	361 ± 53 (UC)	310 ± 30 (UC)
14	400 ± 7 (0.42)	238 ± 6 (Mixed)	262 ± 39 (UC)
16	433 ± 60 (0.31)	398 ± 81 (Mixed)	525 ± 64 (UC)
18	512 ± 37 (0.37)	554 ± 70 (UC)	452 ± 26 (UC)
19	325 ± 9 (0.37)	126 ± 34 (Mixed)	355 ± 47 (UC)

^aLigand efficiency was calculated using the equation LE = (1.37 × pIC₅₀)/HA, where HA means heavy atom, i.e., a non-hydrogen atom.

^bUC: Uncompetitive inhibition.

provided an array of hits with IC₅₀ ranging from 325 μM to 674 μM and ligand efficiencies from 0.31 to 0.42. The inhibition constant [K_i] with respect to both substrates IMP and NAD⁺ was determined by assaying various concentrations of each inhibitor with five different concentrations of substrate and a fixed saturating concentration of the cosubstrate. The inhibition data for these fragments are summarized in Table 2. All compounds yielded an uncompetitive inhibition pattern with respect to NAD⁺ with K_i values ranging from 262 to 525 μM. Fragments 14, 16, and 19 yielded a mixed inhibition with respect to IMP with K_i values ranging from 126 to 398 μM, and compounds 1, 2, 11, and 18 yielded an uncompetitive inhibition with K_i values ranging from 361 to 609 μM.

Inhibition constants of compound 2 toward full-length *Mth* IMPDH were also determined. Compound 2 inhibited full-length *Mth* IMPDH enzyme with a K_i value of 572 ± 14 μM with IMP as the substrate and a K_i value of 534 ± 18 μM with NAD as the substrate, which are similar to the K_i values observed for the *Mth* IMPDH ΔCBS enzyme.

X-ray Structure of Compounds 1 (7759844) and 2. Compound 1 and the six fragment hits (2, 11, 14, 16, 18, and 19) were selected for structural characterization using X-ray crystallography by soaking into preformed crystals of *Mth* IMPDH ΔCBS as previously described.²⁰ After molecular replacement, clear electron density was observed in the 2F₀ – F_c difference map (σ = 3.0) for IMP, and in addition density was observed for one molecule of compound 1 (Figure 3A) and two molecules of compound 2 (Figure 3B), which were partially occupying the NAD⁺ binding site. None of the other fragments

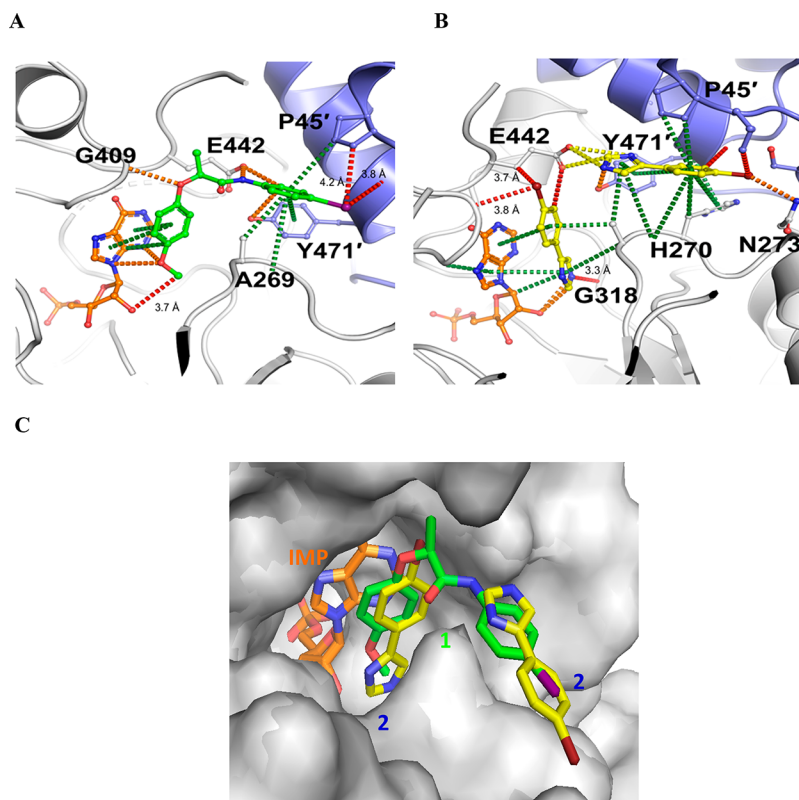


Figure 3. X-ray crystal structure of compounds 1 and 2 bound to *Mth* IMPDH ΔCBS. Ligand interactions are represented as dotted lines; hydrogen bonds are represented in red, polar interactions in orange, ionic interactions in yellow, and aromatic and π interactions in green dotted lines. Protein–ligand interactions were analyzed using Arpeggio. (a) Interactions made by 1 (green) in the X-ray crystal structure of the complex of IMPDH with IMP (orange). (b) Interactions made by 2 (yellow) in the X-ray crystal structure of the complex of IMPDH with IMP. (c) Structural alignment of the IMPDH crystal structures of 1 (green) and 2 (yellow).

(11, 14, 16, 18, and 19) showed any electron density in the X-ray crystal structures. Although the kinetic studies of compounds 1 and 2 suggested that these two compounds are uncompetitive with respect to NAD⁺, the binding mode of compounds 1 and 2 closely resembles that of other previously reported uncompetitive inhibitors of *Mtb* IMPDH.^{21,24,25} It has been proposed that the uncompetitive mode of inhibition of IMPDH inhibitors with respect to NAD⁺ is consistent with their binding preferentially to the covalent IMPDH-XMP* intermediate after NADH has been released.^{24,25,33}

The structure of *Mtb* IMPDH ΔCBS with compound 1 showed that the inhibitor binds in the NAD pocket in a near identical manner to our recently described IMPDH inhibitors.^{24,25} Compound 1 formed strong π interactions with the hypoxanthine group of IMP, P45', Y471', and polar interactions with G409, E442, P45', and G470'. The electron density revealed two molecules of compound 2 within the NAD binding pocket of IMPDH. One molecule of compound 2 stacked with IMP, forming extensive π interactions with the hypoxanthine group of IMP. This fragment was further stabilized through polar interactions, hydrogen bonds, and π interactions to surrounding residues in the active site pocket, including A269, G318, and E442. The other molecule of compound 2 sits closer to the opening of the active site, making polar interactions with N273 and E442, and π interactions with H270 and Y471'.

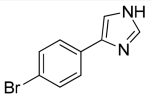
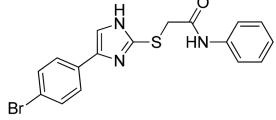
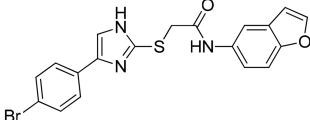
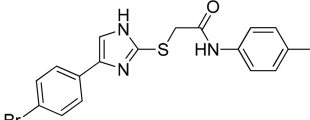
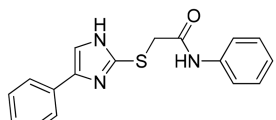
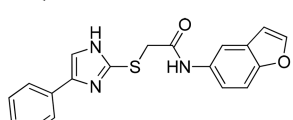
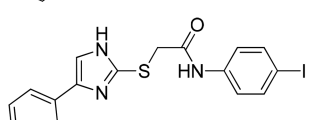
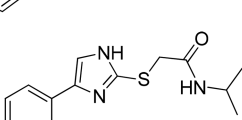
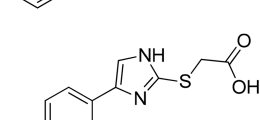
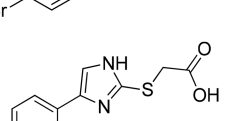
A comparison of the structure of *Mtb* IMPDH ΔCBS with compound 1 with the fragment 2 structure shows that the two molecules of 2 mimic the position of the larger inhibitor 1 (Figure 3C).

Fragment Elaboration. Fragment 2 was selected as the starting point for exploration because of the ease of synthetic modification and the availability of a X-ray crystal structure to guide the optimization. For chemical elaboration of 2, fragment linking as well as fragment growing were considered. As the two molecules of fragment 2 are found to bind in adjacent regions of the target protein, the fragment-linking approach was the more attractive option. However, before fragment linking, fragment 2 was further optimized with the aim of improving the binding affinity. The structures and inhibitory activities of these compounds against *Mtb* IMPDH ΔCBS are summarized in Tables 3 and 4. The corresponding data for fragment 2 have also been included for comparative purposes.

All compounds were evaluated at a concentration of 100 μ M with *Mtb* IMPDH ΔCBS.

Fragment Growing. The fragment-growing strategy involves using structure-based drug design to form additional interactions by growing out from the starting fragment. Fragment 2 was modified at the 2-position of the imidazole ring to explore the introduction of various aromatic rings linked by a thioacetamide (20–22) to form π interactions with the hypoxanthine group of IMP (Figure S1). Such modifications gave compounds with improved *Mtb* IMPDH ΔCBS inhibition. The phenyl and benzofuran derivatives (20 and 21) showed 13 and 31% inhibition, respectively. *Mtb* IMPDH ΔCBS inhibition was shown to be sensitive to minor modifications of the phenyl substituent groups; for example, the 4-iodo substituted 22 showed 30% inhibition at 100 μ M, whereas the unsubstituted compound, 20, showed 13% inhibition at the same concentration. The effect of the removal of the 4-bromo group was investigated and compounds 23–25 were synthesized. Removal of the bromo substituent in compounds 20–22 (13–31% inhibition at 100 μ M) was tolerated (23–25, 3–46% inhibition at 100 μ M). The importance of the aromatic amide linked by a

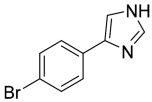
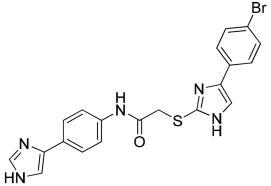
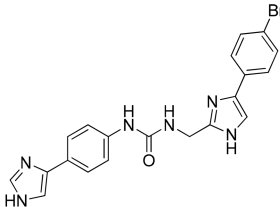
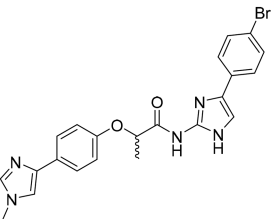
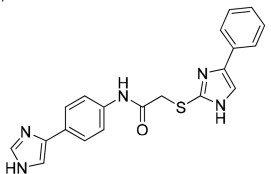
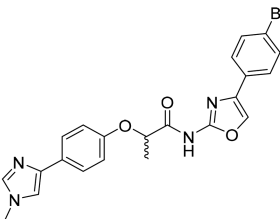
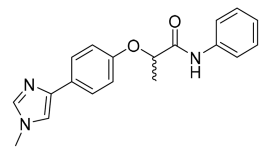
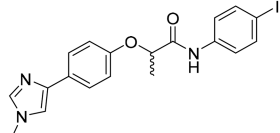
Table 3. Structures and Activities for Fragment 2 and Compounds 20–28 against *Mtb* IMPDH ΔCBS

Compd	Structure	% Inhibition at 100 μ M
2		< 5%
20		13 \pm 3
21		31 \pm 6
22		30 \pm 3
23		< 5%
24		36 \pm 1
25		46 \pm 3
26		< 5%
27		< 5%
28		< 5%

thioacetamide was subsequently examined. Replacing the phenyl with isopropyl (26) resulted in complete loss of activity. Substitution of the thioacetamide by a thioacetic acid also led to a complete loss in activity (compounds 27 and 28).

Fragment Linking and SAR. Examination of the X-ray crystal structure of the previously reported inhibitor 1 when overlaid with fragment 2 revealed that the distance between the 4-position of the phenyl ring of fragment 2 and the 2-position of the imidazole ring represents the closest approach of the molecules (Figure S1). On the basis of this structural

Table 4. Structures and Activities for Fragment 2 and Compounds 29–35 against *Mth* IMPDH Δ CBS

Compd	Structure	% Inhibition at 100 μ M	IC ₅₀ (μ M) (LE) ^a
2		< 5%	674 \pm 53 (0.36)
29		20 \pm 5	ND ^b
30		56 \pm 11	58 \pm 8 (0.21)
31		99 \pm 11 ^c	0.52 \pm 0.004 (0.29)
32		24 \pm 1	ND
33		83 \pm 2 ^c	2.21 \pm 0.08 (0.26)
34		4 \pm 1 ^c	ND
35		97 \pm 1 ^c	0.47 \pm 0.03 (0.34)

^aLigand efficiency was calculated using the equation $LE = (1.37 \times pIC_{50})/HA$, where HA means heavy atom, i.e., a non-hydrogen atom. ^bND: not determined. IC₅₀ values were determined for compounds that showed >50% inhibition. ^c%Inhibition at 10 μ M.

information, three different linkers were designed to connect the two copies of the fragment 2 at these positions (compounds 29–31). Initially, a thioacetamide and urea linker moieties were examined. Compounds 29 and 30 showed 20% and 56% of *Mth* IMPDH Δ CBS inhibition, respectively, at 100 μ M (Table 4). Interestingly, compound 30 showed a 12-fold improvement in

Mth IMPDH Δ CBS inhibitory activity with an IC₅₀ of 58 μ M, compared to the fragment 2.

The lactate linker was then used, but all attempts to link 4-phenylimidazole with 4-(4-bromophenyl)-1H-imidazole were unsuccessful. We therefore decided to synthesize compound 31, which contains 1-methyl-4-phenyl-1H-imidazole and 4-(4-

bromophenyl)-1*H*-imidazole linked with a lactate analogue, as in compound **1**. Compound **31** (Table 4) showed markedly improved *Mth* IMPDH Δ CBS inhibition with a LE of 0.29 and IC_{50} of 0.52 μ M, which is 1300-fold more potent compared to the fragment **2**. Although compound **31** binds in the cofactor site, the mechanism of inhibition can vary depending on its relative affinities for the E·IMP and E·XMP* complexes.^{8,11} Kinetic evaluation of compound **31** showed the mode of *Mth* IMPDH Δ CBS inhibition was uncompetitive with respect to both IMP and the NAD^+ cofactor (see Figure S2, Supporting Information) with a K_i value of $0.30 \pm 0.02 \mu$ M with IMP as the substrate and a K_i value of 0.20 ± 0.01 with NAD as the substrate.

Inhibition constants of compound **31** toward full-length *Mtb* IMPDH were also determined. Compound **31** inhibited full-length *Mtb* IMPDH enzyme with a K_i value of $0.61 \pm 0.05 \mu$ M with IMP as the substrate and a K_i value of $0.39 \pm 0.02 \mu$ M with NAD as the substrate. The inhibition constants were consistent with the data using the *Mth* IMPDH Δ CBS enzyme.

Removal of the bromo substituent in compound **29** to give compound **32** was well tolerated (Table 4). The importance of the imidazole group for the inhibitory activity against *Mth* IMPDH Δ CBS was confirmed by replacing of the 4-(4-bromophenyl)-1*H*-imidazole substituent of compound **31** with 4-(4-bromophenyl)oxazole (**33**) which resulted in a 4-fold loss of activity (Table 4). Replacing the 4-(4-bromophenyl)-1*H*-imidazole of **31** by a phenyl (**34**) resulted in complete loss of activity (Table 4). However, the 4-iodophenyl derivative **35** demonstrated slightly improved activity ($IC_{50} = 0.47 \mu$ M, LE = 0.34) compared to compounds **31** ($IC_{50} = 0.52 \mu$ M, LE = 0.29) and **1** ($IC_{50} = 0.77 \mu$ M, LE = 0.40). It is noteworthy that LE of compound **35** was comparable to that of the original fragment hit **2** (LE = 0.36) and other reported IMPDH inhibitors.³⁴

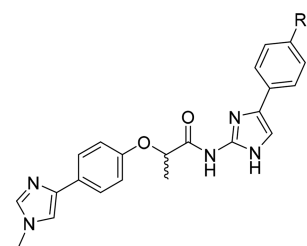
The importance of the 4-bromo substituent on the phenyl ring in compound **31** was also explored (compounds **36–39**, Table 5). Removal of the bromo substituent (**36**) resulted in a 5-fold loss in activity, whereas replacing this group with an iodine (**39**) or a morpholine ring (**37**) resulted in less than 1.3-fold loss in activity. The electronic nature of the substituent in this position had little effect on inhibitory activity. For example, an electron-donating methoxy (**38**) retained activity comparable to that of the bromine derivative (**31**). Among them, imidazoles **31**, **37–38**, and **39** were found to be potent inhibitors of *Mth* IMPDH Δ CBS with IC_{50} values ranging from 520 to 690 nM.

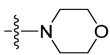
The (*S*)-isomer of **31** was found to bind preferentially (Table 5), with the racemate **31** having approximately half the *Mth* IMPDH Δ CBS inhibition of the (*S*)-isomer **31**. This observation accords with the results previously reported for other series of IMPDH inhibitors.^{21,35}

X-ray Structure of Compound 31. From crystals soaked with compound **31**, the $2F_0 - F_c$ difference map ($\sigma = 3.0$) revealed strong density for the inhibitor. The structure of compound **31** (Figure 4A) showed that it bound in a nearly identical manner to compounds **1** and **2** in the NAD binding pocket (Figure 4B), stacking with IMP, and maintaining the interactions with H270, N273, E442, and P45 and Y471 from the neighboring subunit. Compound **31** made additional interactions in the binding pocket, including polar interactions with D267 and N297.

Whole-Cell Activity against *Mtb*. The whole-cell activity of the most potent analogues **31**, **33–39**, and (*S*)-**31** *in vitro* was determined against *Mtb* H37Rv (see Table S1, Supporting Information). No significant inhibition of bacterial growth was detected for any of the compounds ($MIC_{90} \geq 50 \mu$ M) over the

Table 5. Structures and Activities for Compounds 31, 36–39, and (*S*)-31 against *Mth* IMPDH Δ CBS



Compd	R ₁	% Inhibition at 10 μ M	IC_{50} (μ M) (LE) ^a
31	Br	99 \pm 1	0.52 \pm 0.004 (0.29)
36	H	77 \pm 3	2.76 \pm 0.21 (0.26)
37		94 \pm 1	0.52 \pm 0.01 (0.24)
38	OMe	95 \pm 1	0.64 \pm 0.03 (0.27)
39	I	96 \pm 1	0.69 \pm 0.06 (0.28)
(<i>S</i>)- 31	Br	99 \pm 1	0.27 \pm 0.02 (0.30)

^aLigand efficiency was calculated using the equation $LE = (1.37 \times pIC_{50})/HA$, where HA means heavy atom, i.e., a non-hydrogen atom.

tested concentration range (0–100 μ M). There are currently ongoing efforts to explain the lack of efficacy of the potent *Mth* IMPDH Δ CBS inhibitors described which could be caused by low membrane permeability, poor metabolic stability, and/or drug-efflux mechanisms.

Synthetic Chemistry. Compounds **20–29** and **32** were synthesized from 4-phenyl-1*H*-imidazole-2-thiol or 4-(4-bromophenyl)-1*H*-imidazole-2-thiol according to the sequence described in Scheme 1. Thioacetic derivatives **27** and **28** were prepared by treatment of 4-phenyl-1*H*-imidazole-2-thiol or 4-(4-bromophenyl)-1*H*-imidazole-2-thiol with 2-chloroacetic acid in the presence of NaOH followed by neutralization with hydrochloric acid.

Thioacetamide **26** was synthesized by amide coupling between thioacetic derivative **28** and isopropylamine. Similarly, thioacetamides **20–25**, **29**, and **32** were prepared by cross-linking 4-phenyl-1*H*-imidazole-2-thiol or 4-(4-bromophenyl)-1*H*-imidazole-2-thiol with α -chloroacetamides **40–43**, which were obtained by acylation of anilines with various substituents with chloroacetyl chloride.

The synthesis of urea **30** was achieved as shown in Scheme 2 by coupling amine **44** and *N*-(4-(1*H*-imidazol-4-yl)phenyl)-1*H*-imidazole-1-carboxamide, which was obtained from commercially available 4-(1*H*-imidazol-4-yl)aniline as a crude intermediate, in the presence of *N,N*-diisopropylethylamine. Amine **44** was synthesized from benzyl ((5-(4-bromophenyl)-1*H*-imida-

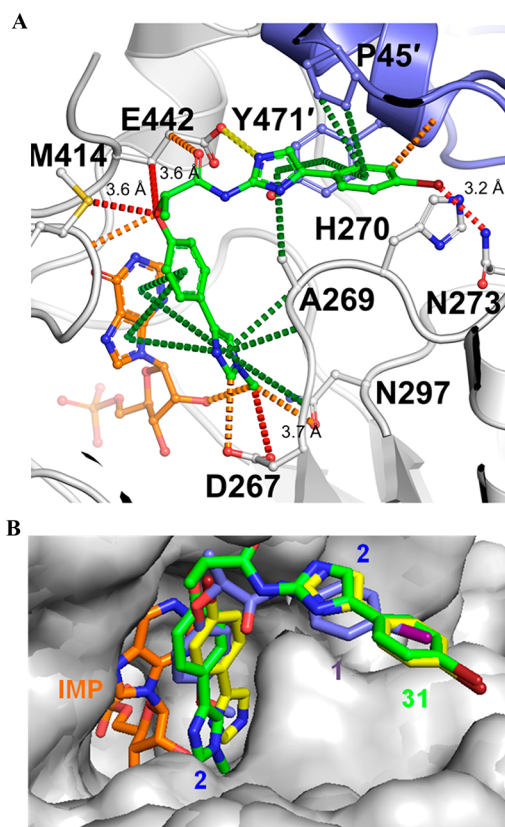
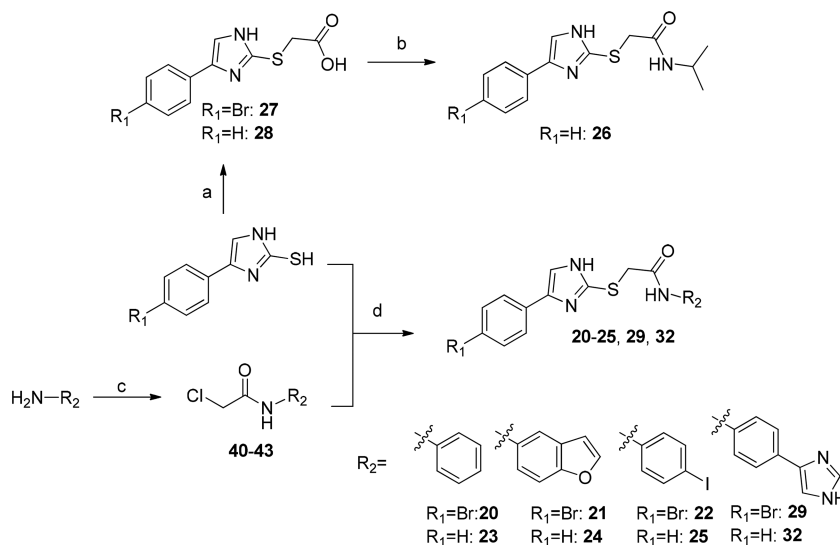


Figure 4. X-ray crystal structure of compound 31 bound to *Mth* IMPDH Δ CBS. Protein–ligand interactions were analyzed using Arpeggio. (a) Interactions made by 31 in the X-ray crystal structure of the complex of IMPDH with IMP (orange). Ligand interactions are represented as dotted lines; hydrogen bonds are represented in red, polar interactions in orange, ionic interactions in yellow, and aromatic and π interactions in green dotted lines. (b) Structural alignment of the IMPDH crystal structures of 1 (lilac), 2 (yellow), and 31 (green).

zol-2-yl)methyl)carbamate,³⁶ followed by the deprotection of the benzyloxycarbonyl group under acidic condition.

Scheme 1. Synthesis of Thioacetamide and Thioacetic Derivatives 20–29 and 32^a



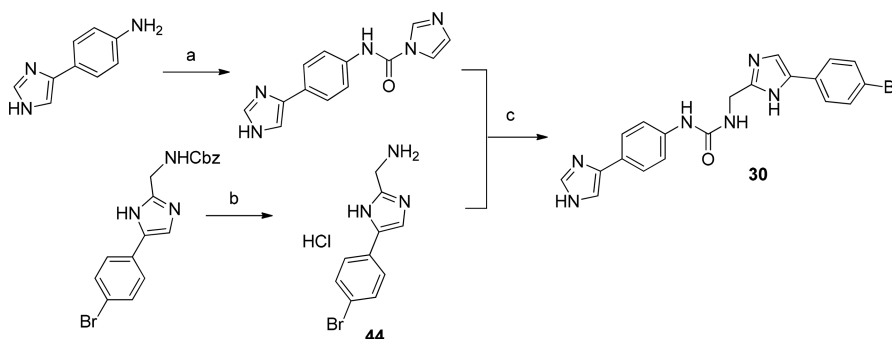
^aReagent and conditions: (a) 2-chloroacetic acid, NaOH, EtOH, 80 °C, 69–72%; (b) isopropylamine, HATU, DIPEA, EtOAc, rt, 73%; (c) chloroacetyl chloride, TEA, DCM, rt, 89–99%; (d) NaOH, MeOH, H₂O, 70 °C, 69–96%.

Imidazole derivatives 31, 36–38, and 39 were prepared following the synthetic procedure outlined in Scheme 3. 2-Aminoimidazoles 50–54 were synthesized according to a published microwave-assisted protocol.³⁷ In brief, 2-aminoimidazoles 50–54 were prepared by reaction of the commercially available α -haloketones and *N*-acetylguanidine, followed by deacetylation (Scheme 3). Acid 59 was synthesized starting with imidazole 55, which was prepared by reaction of 2-bromo-4'-hydroxyacetophenone with formamide as reported previously.³⁸ The phenol 57 was synthesized by alkylation of imidazole 55, followed by deprotection of the methyl ether with BBr₃. Substituted phenol 57 was converted to the ether 58 upon treatment with methyl 2-bromopropionate in the presence of Cs₂CO₃. Enantiomerically pure phenyl ethers were synthesized by using Mitsunobu reaction conditions with ethyl *D*-lactate (Scheme 4). After the hydrolysis of the ester group, the resulting carboxylic acid 59 was treated with thionyl chloride to give the acid chloride 60, which was reacted with 2-aminoimidazoles 50–54 to afford imidazole derivatives 31, 36–38, and 39.

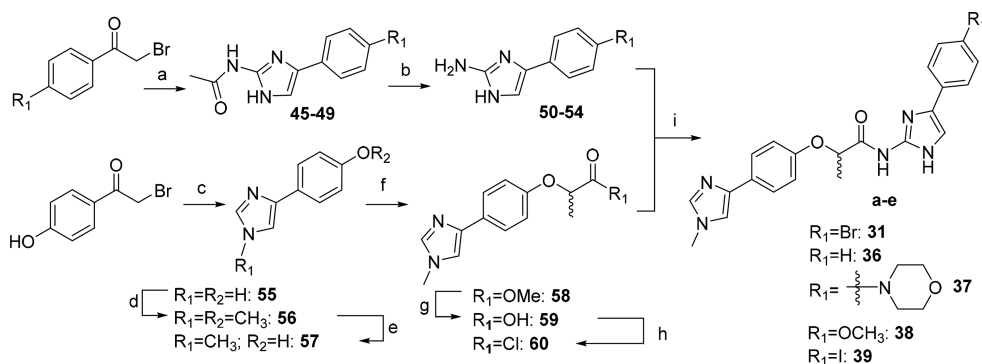
The syntheses of 2-acylaminooxazole 33 and amides 34–35 were achieved as shown in Scheme 5. 2-Acylaminooxazole derivative 33 was obtained by coupling the acid chloride derivative 60 with 2-aminooxazole derivative 61, which was prepared by reaction of 2,4'-dibromoacetophenone with urea. Similarly, amides 34–35 were prepared by coupling the corresponding anilines with the acid chloride derivative 60.

CONCLUSIONS

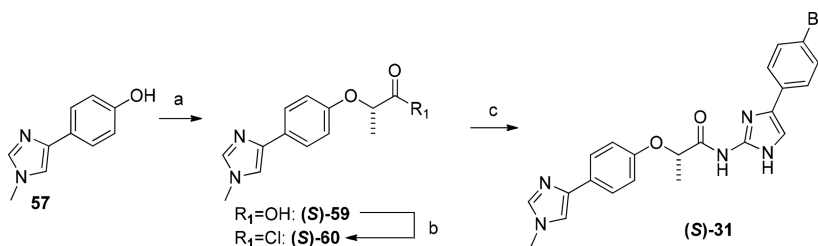
FBDD has emerged as a robust approach to identify small molecules that bind to a wide range of therapeutic targets. Fragment elaboration strategies have resulted in the development of a number of compounds that have progressed into clinical trials. Within the area of TB drug discovery, a number of HTS and phenotypic screens have been performed during the past decade. Although HTS identified a number of leads that show high potency *in vitro*, the translation to an *in vivo* effect has proven challenging.

Scheme 2. Synthesis of Urea 30^a

^aReagent and conditions: (a) CDI, THF, rt, quant.; (b) HCl (4 M), dioxane, 100 °C, quant.; (c) DIPEA, DMF, rt, 26%.

Scheme 3. Synthesis of 2-Acylaminoimidazole Derivatives 31, 36–38, and 39^a

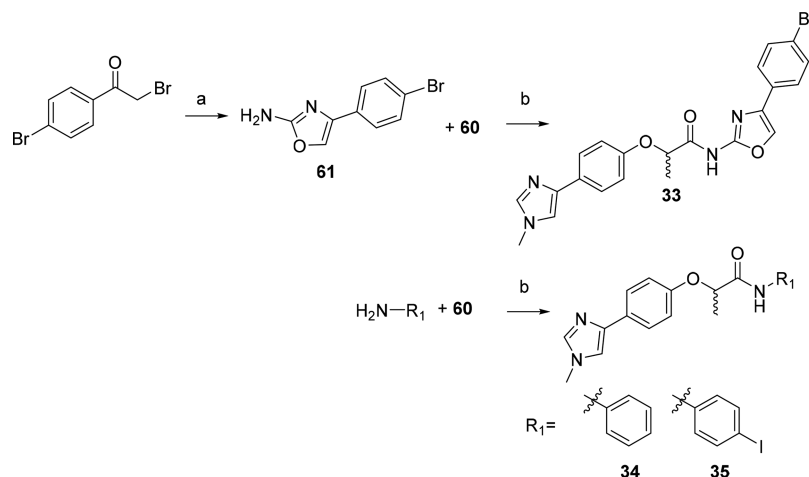
^aReagent and conditions: (a) acetylguanidine, CH₃CN, μ W, 100 °C, 71–88%; (b) (1) 20% H₂SO₄, MeOH:H₂O (1:1 v/v), μ W, 100 °C; (2) aq Na₂CO₃, 79–95%; (c) formamide, 150 °C, 99%; (d) CH₃I, Cs₂CO₃, DMF, rt, 88%; (e) BBr₃ (1 M in DCM), –78 °C to rt, DCM, 96%; (f) Cs₂CO₃, methyl 2-bromopropionate, DMF, 60 °C, 92%; (g) NaOH, THF:H₂O (2:1 v/v), 80 °C, 65%; (h) SOCl₂, 80 °C, quant.; (i) TEA, DCM, 40 °C, 61–72%.

Scheme 4. Synthesis of the S-Enantiomer of 31^a

^aReagent and conditions: (a) (1) Ethyl D-lactate, PPh₃, DEAD, THF, rt; (2) NaOH, THF:H₂O (2:1 v/v), rt, 56%; (b) SOCl₂, 80 °C, quant.; (c) 50, TEA, DCM, 40 °C, 69%.

This study illustrates the successful application of a fragment-based approach followed by fragment optimization to obtain nanomolar affinity ligands of IMPDH. A library of 960 fragments were screened against *Mth* IMPDH Δ CBS, and from the screen the phenylimidazole fragment hit **2** (IC₅₀ = 674 μ M) was identified. Kinetic experiments showed that **2** was an uncompetitive inhibitor of *Mth* IMPDH Δ CBS with respect to NAD⁺ and IMP. Two molecules of the fragment **2** were shown to bind at the NAD binding site of the enzyme. The X-ray crystal structure also revealed that one molecule of fragment **2** makes π interactions with IMP and the other molecule sits closer to the opening of the active site, making polar interactions with N273 and E442 and π interactions with H270 and Y471'. This provides potential for further optimization of fragment **2**. To explore better the possibilities given by fragment **2**, fragment-linking and

fragment-growing strategies were employed, resulting in low micromolar to nanomolar affinity compounds. Among them, compounds **31**, **35**, and **37–39** were the most potent IMPDH inhibitors of the series described in this work with IC₅₀ values between 0.47 and 0.69 μ M, which represent >1000-fold improvement in *Mth* IMPDH Δ CBS potency over the initial fragment hit. Compound **31** was shown to bind at the NAD binding site of the enzyme, and the X-ray crystal structure also revealed that it makes π interactions with IMP, maintaining the interactions with H270, N273, E442, and P45 and Y471 from the neighboring subunit. Moreover, compound **31** made additional interactions in the binding pocket, including polar interactions with D267 and N297. A comparison of this structure with the fragment **2** structure shows that the two molecules of **2** mimic the position of the larger inhibitor **31**. This is the first example of

Scheme 5. Synthesis of 2-Acylaminoimidazole Derivative 33 and Amides 34–35^a

^aReagent and conditions: (a) urea, CH₃CN, 80 °C, 78%; (b) TEA, DCM, rt (for 34 and 35) or 40 °C (for 33), 64–76%.

utilizing the fragment-based approach specifically to identify new potent inhibitors of IMPDH. Further structural optimization to improve the cellular activity of these analogues is ongoing with the aim of developing novel classes of anti-TB agents.

EXPERIMENTAL SECTION

1. Chemistry. 1.1. General Experimental Methods. Solvents were distilled prior to use and dried by standard methods. Unless otherwise stated, ¹H and ¹³C NMR spectra were obtained in CDCl₃, MeOD, or DMSO-*d*₆ solutions using either a Bruker 400 MHz AVANCE III HD Smart Probe, 400 MHz QNP cryoprobe, or 500 MHz DCH cryoprobe spectrometer. Chemical shifts (δ) are given in ppm relative to the residual solvent peak (CDCl₃; ¹H, δ = 7.26 ppm; ¹³C, δ = 77.16 ppm), and the coupling constants (*J*) are reported in hertz (Hz). Optical rotations were measured on a PerkinElmer Polarimeter 343 at 589 nm (Na D-line), and specific rotations are reported in 10⁻¹ deg cm² g⁻¹. Microwave reactions were performed using a Biotage Initiator system under reaction conditions as indicated for each individual reaction.

Reactions were monitored by TLC and LCMS to determine consumption of starting materials. Flash column chromatography was performed using an Isolera Spektra One/Four purification system and the appropriately sized Biotage SNAP column containing KP-silica gel (50 μ m). Solvents are reported as volume/volume eluent mixture where applicable.

High resolution mass spectra (HRMS) were recorded using a Waters LCT Premier Time of Flight (TOF) mass spectrometer or a Micromass Quadrupole-Time of Flight (Q-TOF) spectrometer.

Liquid chromatography mass spectrometry (LCMS) was carried out using an Ultra Performance Liquid Chromatographic system (UPLC) Waters Acquity H-class coupled to a Waters SQ Mass Spectrometer detector. Samples were detected using a Waters Acquity TUV detector at 2 wavelengths (254 and 280 nm). Samples were run using an Acquity UPLC HSS column and a flow rate of 0.8 mL/min. The eluent consisted of 0.1% formic acid in water (A) and acetonitrile (B); gradient, from 95% A to 5% A over a period of 4 or 7 min.

All final compounds had a purity greater than 95% by LCMS analysis.

General Method A: Synthesis of Thioacetamides 20–25, 29, and 32. To a solution of the 2-chloroacetamide derivative (0.17 mmol) in MeOH (8 mL) was added 4-(4-bromophenyl)-1H-imidazole-2-thiol or 4-phenyl-1H-imidazole-2-thiol (0.17 mmol), followed by a solution of NaOH (0.67 mmol) in H₂O (2.5 mL). The reaction mixture was stirred at 70 °C for 3 h. After cooling to rt, the solvents were removed *in vacuo* and the resulting residue was taken up in 30 mL of EtOAc and washed with H₂O (15 mL). The aqueous layer was extracted with EtOAc (3 \times 30 mL) and the combined organic layers were washed with brine and dried over MgSO₄. Filtration and evaporation afforded crude products, which were purified as indicated below.

General Method B: Synthesis of Thioacetic Derivatives 27 and 28.

A solution of 4-phenyl-1H-imidazole-2-thiol or 4-(4-bromophenyl)-1H-imidazole-2-thiol (2.80 mmol) and NaOH (5.0 mmol) in EtOH (5 mL) was reflux for 1 h. After cooling to rt, a solution of 2-chloroacetic acid (2.80 mmol) in EtOH (2 mL) was added. The reaction was stirred at reflux for an additional 3 h and then cooled to 0 °C. The reaction mixture was diluted with cold water (5 mL) and acidified with 1 M HCl. The precipitated product was collected by filtration and washed with DCM (2 \times 2 mL).

General Method C: Synthesis of Compounds 31, 33, and 36–39. A mixture of acid 59 (0.20 mmol) and SOCl₂ (2 mL) was heated at 80 °C for 2 h. The solvent was removed under reduced pressure to give the acid chloride 60 as a white solid. The resulting solid was immediately dissolved in anhydrous DCM, and the resulting solution was added slowly dropwise at 0 °C to a solution of the corresponding substituted 2-aminoimidazoles (0.20 mmol) and TEA (0.80 mmol) in anhydrous DCM (5 mL). The reaction mixture was stirred at 40 °C for 36 h and then diluted with DCM (20 mL) and washed with saturated aqueous NaHCO₃. The aqueous phase layer was then extracted with DCM (2 \times 20 mL), and the combined organic layers were dried over MgSO₄ and filtered, and the solvent was removed under reduced pressure to afford a yellow oil, which was purified by flash chromatography, eluting with the solvent system specified.

General Method D: Synthesis of Amides 34–35. A mixture of acid 59 (0.20 mmol) and SOCl₂ (2 mL) was heated at 80 °C for 2 h. The solvent was removed under reduced pressure to give 60 as a white solid. The resulting solid was immediately dissolved in anhydrous DCM, and the resulting solution was added slowly dropwise at 0 °C to a solution of the corresponding aniline (0.20 mmol) and triethylamine (0.80 mmol) in anhydrous DCM (5 mL). The reaction mixture was stirred at rt for 4 h and then diluted with DCM (20 mL) and washed with saturated aqueous NaHCO₃. The aqueous phase layer was then extracted with DCM (2 \times 20 mL), and the combined organic layers were dried over MgSO₄ and filtered, and the solvent was removed under reduced pressure to afford a yellow oil, which was purified by flash chromatography, eluting with the solvent system specified.

General Method E: Synthesis of α -Chloroacetamides 40–43. Et₃N (4.77 mmol) followed by a solution of chloroacetyl chloride (4.77 mmol) in DCM (3 mL) were added to a stirred solution of the corresponding aniline (4.38 mmol) in DCM (5 mL) at rt. The reaction mixture was stirred at rt for 2–4 h. The reaction was then diluted with DCM (20 mL) and washed with saturated aqueous NaHCO₃, 1 M HCl, and brine and dried over anhydrous MgSO₄, and the solvent was removed under reduced pressure. Compound 43 was purified by flash chromatography eluting with the solvent system specified, although other analogues were used in subsequent reactions without further purification.

General Method F: Synthesis of Substituted *N*-(1*H*-imidazol-2-yl)acetamides 45–49. A mixture of the corresponding 2-bromoacetophenone derivative (0.38 mmol) and acetylguanidine (1.13 mmol) in anhydrous acetonitrile (3 mL) was heated at 100 °C using microwave irradiation for 15 min. The solvent was removed, and the residue was taken in H₂O (3 mL) and filtered, and the solid was washed with H₂O (2 mL × 2) and DCM (2 mL). The solid obtained was used in the next step without further purification.

General Method G: Synthesis of Substituted 2-Aminoimidazoles 50–54. To a solution of the corresponding substituted *N*-(1*H*-imidazol-2-yl)acetamides (0.31 mmol) in a 1:1 v/v mixture of MeOH and H₂O (2.4 mL) was added concentrated H₂SO₄ (0.6 mL), and the reaction mixture was heated at 100 °C under microwave irradiation for 15–30 min. The reaction mixture was concentrated, and the resulting residue was resuspended in H₂O (5 mL), and a saturated aqueous Na₂CO₃ was added until pH 8. The product was extracted into EtOAc (3 × 40 mL). The combined organic fractions were dried over MgSO₄, and the solvent was removed under reduced pressure. The resulting solid was used in the next reaction without further purification.

2-((4-(4-Bromophenyl)-1*H*-imidazol-2-yl)thio)-*N*-phenylacetamide (20). Compound 40 (29 mg, 0.17 mmol) was reacted with 4-(4-bromophenyl)-1*H*-imidazole-2-thiol (43 mg, 0.17 mmol) according to general method A. Purification by flash chromatography (1–20% v/v MeOH in DCM) afforded 20 (59 mg, 0.15 mmol, 89% yield) as a white solid. ¹H NMR (400 MHz, MeOD) δ 7.62 (br s, 2H), 7.56–7.39 (m, 5H), 7.36–7.17 (m, 2H), 7.13–7.00 (m, 1H), 3.82 (s, 2H) ppm. ¹³C NMR (100 MHz, MeOD) δ 169.6, 141.3, 139.6, 132.8, 129.8, 129.8, 127.5, 125.5, 121.4, 121.2, 121.2, 116.7, 39.6 ppm. LCMS (ESI[−]) *m/z* 388.0 [M − H][−], retention time 2.20 min (100%). HRMS (ESI⁺): *m/z* calculated for C₁₇H₁₅BrN₃OS [M + H]⁺: 388.0119. Found: 388.0121.

***N*-(Benzofuran-5-yl)-2-((4-(4-bromophenyl)-1*H*-imidazol-2-yl)thio)acetamide (21).** Compound 41 (36 mg, 0.17 mmol) was reacted with 4-(4-bromophenyl)-1*H*-imidazole-2-thiol (43 mg, 0.17 mmol) according to general method A. Purification by flash chromatography (1–20% v/v MeOH in DCM) afforded 21 (70 mg, 0.16 mmol, 96% yield) as a white solid. ¹H NMR (400 MHz, DMSO-*d*₆) δ 12.50 (br s, 1H), 10.35 (br s, 1H), 7.94 (dd, *J* = 10.6, 2.0 Hz, 2H), 7.73–7.64 (m, 2H), 7.52–7.44 (m, 4H), 7.34 (dd, *J* = 8.8, 2.2 Hz, 1H), 6.91 (dd, *J* = 2.2, 1.0 Hz, 1H), 3.99 (s, 2H) ppm. ¹³C NMR (100 MHz, DMSO-*d*₆) δ 166.5, 150.8, 146.7, 140.2, 139.9, 134.3, 133.6, 131.4, 127.4, 126.2, 119.0, 116.9, 115.7, 111.6, 111.3, 107.0, 37.9 ppm. LCMS (ESI[−]) *m/z* 428.0 [M − H][−], retention time 2.22 min (100%). HRMS (ESI⁺): *m/z* calculated for C₁₉H₁₅BrN₃O₂S [M + H]⁺: 428.0068. Found: 428.0065.

2-((4-(4-Bromophenyl)-1*H*-imidazol-2-yl)thio)-*N*-(4-iodophenyl)acetamide (22). Compound 42 (50 mg, 0.17 mmol) was reacted with 4-(4-bromophenyl)-1*H*-imidazole-2-thiol (43 mg, 0.17 mmol) according to general method A. Purification by flash chromatography (1–20% v/v MeOH in DCM) afforded 22 (60 mg, 0.11 mmol, 69% yield) as a white solid. ¹H NMR (500 MHz, MeOD) δ 7.63–7.58 (m, 4H), 7.56–7.45 (m, 3H), 7.38–7.31 (m, 2H), 3.81 (s, 2H) ppm. ¹³C NMR (125 MHz, MeOD) δ 169.6, 139.6, 138.9, 132.7, 127.5, 127.1, 123.0, 116.6, 111.4, 88.1, 39.7 ppm. LCMS (ESI[−]) *m/z* 511.7 [M − H][−], retention time 2.30 min (100%). HRMS (ESI⁺): *m/z* calculated for C₁₇H₁₄BrI₂N₃O₂S [M + H]⁺: 513.9086. Found: 513.9087.

***N*-Phenyl-2-((4-phenyl-1*H*-imidazol-2-yl)thio)acetamide (23).** Compound 40 (42 mg, 0.25 mmol) was reacted with 4-phenyl-1*H*-imidazole-2-thiol (44 mg, 0.25 mmol) according to general method A. Purification by flash chromatography (1–20% v/v MeOH in DCM) afforded 23 (61 mg, 0.20 mmol, 82% yield) as a white solid. ¹H NMR (500 MHz, MeOD) δ 7.71 (br s, 2H), 7.54–7.49 (m, 2H), 7.47 (br s, 1H), 7.35 (t, *J* = 7.4 Hz, 2H), 7.31–7.20 (m, 3H), 7.11–7.03 (m, 1H), 3.83 (s, 2H) ppm. ¹³C NMR (125 MHz, MeOD) δ 168.3, 142.7, 139.5, 138.5, 138.2, 128.4, 128.3, 126.7, 124.4, 124.1, 123.7, 119.8, 38.3 ppm. LCMS (ESI[−]) *m/z* 308.0 [M − H][−], retention time 1.82 min (95%). HRMS (ESI⁺): *m/z* calculated for C₁₇H₁₆N₃O₂S [M + H]⁺: 310.1014. Found: 310.1004.

***N*-(Benzofuran-5-yl)-2-((4-phenyl-1*H*-imidazol-2-yl)thio)acetamide (24).** Compound 41 (36 mg, 0.17 mmol) was reacted with 4-phenyl-1*H*-imidazole-2-thiol (30 mg, 0.17 mmol) according to general method A. Purification by flash chromatography (1–20% v/v MeOH in

DCM) afforded 24 (42 mg, 0.12 mmol, 70% yield) as a white solid. ¹H NMR (500 MHz, MeOD) δ 7.87 (d, *J* = 2.1 Hz, 1H), 7.72 (d, *J* = 2.2 Hz, 1H), 7.68 (d, *J* = 7.7 Hz, 2H), 7.46 (br s, 1H), 7.40 (d, *J* = 8.8 Hz, 1H), 7.37–7.29 (m, 3H), 7.23 (t, *J* = 7.4 Hz, 1H), 6.76 (dd, *J* = 2.2, 0.9 Hz, 1H), 3.84 (s, 2H) ppm. ¹³C NMR (125 MHz, MeOD) δ 169.6, 153.5, 147.4, 140.9, 134.7, 129.8, 129.1, 128.1, 125.8, 118.9, 114.2, 112.1, 107.7, 39.7 ppm. LCMS (ESI[−]) *m/z* 348.0 [M − H][−], retention time 1.81 min (100%). HRMS (ESI⁺): *m/z* calculated for C₁₉H₁₆N₃O₂S [M + H]⁺: 350.0963. Found: 350.0971.

***N*-(4-Iodophenyl)-2-((4-phenyl-1*H*-imidazol-2-yl)thio)acetamide (25).** Compound 42 (74 mg, 0.25 mmol) was reacted with 4-phenyl-1*H*-imidazole-2-thiol (44 mg, 0.25 mmol) according to general method A. Purification by flash chromatography (1–20% v/v MeOH in DCM) afforded 25 (70 mg, 0.16 mmol, 70% yield) as a white solid. ¹H NMR (500 MHz, MeOD) δ 7.66 (d, *J* = 7.7 Hz, 2H), 7.61–7.54 (m, 2H), 7.44 (br s, 1H), 7.38–7.31 (m, 4H), 7.23 (t, *J* = 6.7 Hz, 1H), 3.80 (s, 2H) ppm. ¹³C NMR (125 MHz, MeOD) δ 169.7, 140.8, 139.6, 138.9, 129.8, 128.2, 125.8, 123.0, 88.1, 39.8 ppm. LCMS (ESI[−]) *m/z* 433.9 [M − H][−], retention time 2.13 min (98%). HRMS (ESI⁺): *m/z* calculated for C₁₇H₁₅IN₃O₂S [M + H]⁺: 435.9981. Found: 435.9989.

***N*-Isopropyl-2-((4-phenyl-1*H*-imidazol-2-yl)thio)acetamide (26).** A solution of propan-2-amine (22 μL, 0.25 mmol), 2-((4-phenyl-1*H*-imidazol-2-yl)thio)acetic acid (60 mg, 0.25 mmol), HATU (194 mg, 0.50 mmol), and DIPEA (90 μL, 0.50 mmol) in EtOAc (10 mL) was stirred for 5 h at rt. The reaction mixture was diluted with EtOAc (40 mL) and washed with saturated aqueous NaHCO₃ (20 mL), water (20 mL), and brine (20 mL). The organic layer was dried over MgSO₄ and filtered. The solvent was removed under reduced pressure to give an oil residue, which was purified by flash chromatography (5–100% v/v EtOAc in petroleum ether) to give the desired product as a white solid (50 mg, 0.18 mmol, 73% yield). ¹H NMR (500 MHz, MeOD) δ 7.37 (d, *J* = 7.8 Hz, 2H), 7.14 (s, 1H), 7.05 (t, *J* = 7.7 Hz, 2H), 6.93 (t, *J* = 7.4 Hz, 1H), 3.62 (dt, *J* = 13.1, 6.4 Hz, 1H), 3.00 (s, 2H), 0.78 (d, *J* = 6.6 Hz, 6H) ppm. ¹³C NMR (125 MHz, MeOD) δ 170.3, 141.1, 140.8, 133.7, 129.7, 128.1, 125.7, 119.7, 43.0, 38.8, 22.4 ppm. LCMS (ESI[−]) *m/z* 273.9 [M − H][−], retention time 1.52 min (100%). HRMS (ESI⁺): *m/z* calculated for C₁₄H₁₈N₃O₂S [M + H]⁺: 276.1171. Found: 276.1172.

2-((4-(4-Bromophenyl)-1*H*-imidazol-2-yl)thio)acetic Acid (27). Following general procedure B, from 4-(4-bromophenyl)-1*H*-imidazole-2-thiol (250 mg, 0.98 mmol) was obtained 27 (220 mg, 0.70 mmol, 72% yield) as a white solid. ¹H NMR (400 MHz, MeOD) δ 7.65–7.56 (m, 2H), 7.57–7.39 (m, 3H), 3.80 (s, 2H) ppm. ¹³C NMR (100 MHz, MeOD) δ 172.9, 141.9, 140.2, 132.9, 132.6, 127.5, 121.8, 118.9, 37.4 ppm. LCMS (ESI[−]) *m/z* 311.0 [M − H][−], retention time 1.59 min (98%). HRMS (ESI⁺): *m/z* calculated for C₁₁H₁₀BrN₂O₂S [M + H]⁺: 312.9646. Found: 312.9654.

2-((4-Phenyl-1*H*-imidazol-2-yl)thio)acetic Acid (28). Following general procedure B, from 4-phenyl-1*H*-imidazole-2-thiol (500 mg, 2.80 mmol) was obtained 28 (450 mg, 1.92 mmol, 69% yield) as a white solid. ¹H NMR (500 MHz, MeOD) δ 7.68 (d, *J* = 7.2 Hz, 2H), 7.59 (s, 1H), 7.41 (t, *J* = 7.7 Hz, 2H), 7.32 (t, *J* = 7.4 Hz, 1H), 3.86 (s, 2H) ppm. ¹³C NMR (125 MHz, MeOD) δ 172.7, 141.7, 139.6, 131.6, 130.0, 129.1, 126.0, 118.9, 37.5 ppm. LCMS (ESI⁺) *m/z* 235.1 [M + H]⁺, retention time 1.22 min (100%). HRMS (ESI⁺): *m/z* calculated for C₁₁H₁₁N₂O₂S [M + H]⁺: 235.0541. Found: 235.0536.

***N*-(4-(1*H*-imidazol-4-yl)phenyl)-2-((4-(4-bromophenyl)-1*H*-imidazol-2-yl)thio)acetamide (29).** Compound 43 (40 mg, 0.17 mmol) was reacted with 4-(4-bromophenyl)-1*H*-imidazole-2-thiol (43 mg, 0.17 mmol) according to general method A. Purification by flash chromatography (1–20% v/v MeOH in DCM) afforded 29 (51 mg, 0.12 mmol, 69% yield) as a white solid. ¹H NMR (400 MHz, MeOD) δ 7.72 (d, *J* = 1.1 Hz, 1H), 7.66 (d, *J* = 8.5 Hz, 4H), 7.59–7.47 (m, 5H), 7.40 (br s, 1H), 3.86 (s, 2H) ppm. ¹³C NMR (125 MHz, MeOD) δ 169.4, 141.2, 138.4, 137.0, 132.8, 127.5, 126.2, 121.4, 116.7, 111.4, 39.7 ppm. LCMS (ESI[−]) *m/z* 451.9 [M − H][−], retention time 1.65 min (100%). HRMS (ESI⁺): *m/z* calculated for C₂₀H₁₇BrN₃O₂S [M + H]⁺: 454.0337. Found: 454.0334.

1-(4-(1*H*-imidazol-4-yl)phenyl)-3-((5-(4-bromophenyl)-1*H*-imidazol-2-yl)methyl)urea (30). To a solution of 4-(1*H*-imidazol-4-yl)aniline (50 mg, 0.31 mmol) in THF (5 mL) was added 1,1-carbonyldiimidazole

(76 mg, 0.47 mmol). The mixture was stirred at rt overnight, and then it was filtered. The filter was washed with THF (2 × 3 mL) and the resulting solid (30 mg, 0.12 mmol) was dissolved in DMF (3 mL), and **44** (42 mg, 0.12 mmol) and *N,N*-diisopropylethylamine (74 μL, 0.48 mmol) were added. The reaction mixture was stirred at rt for 14 h, and then it was poured into water, extracted with EtOAc, dried over Na₂SO₄, and concentrated. After cooling to 0 °C, a 1:5 v/v mixture of MeOH and DCM (12 mL) was added and the suspended solid was collected by filtration and dried at vacuum to yield **30** (35 mg, 0.08 mmol, 26% yield) as a white solid. ¹H NMR (500 MHz, DMSO-*d*₆) δ 12.03 (br s, 2H), 8.64 (br s, 1H), 7.73–7.68 (m, 2H), 7.64–7.59 (m, 2H), 7.57 (d, *J* = 1.9 Hz, 1H), 7.52–7.47 (m, 2H), 7.47–7.39 (m, 2H), 7.39–7.32 (m, 2H), 6.58 (br s, 1H), 4.33 (d, *J* = 5.5 Hz, 2H) ppm. ¹³C NMR (125 MHz, DMSO-*d*₆) δ 155.5, 146.9, 140.6, 138.9, 138.9, 135.9, 134.6, 131.7, 128.8, 126.6, 125.1, 125.0, 119.0, 118.4, 118.2, 113.7, 111.7, 37.6 ppm. LCMS (ESI⁻) *m/z* 437.0 [M - H]⁻, retention time 5.07 min (97%). HRMS (ESI⁺): *m/z* calculated for C₂₀H₁₈BrN₆O [M + H]⁺: 437.0725. Found: 437.0725.

N-(4-(4-Bromophenyl)-1*H*-imidazol-2-yl)-2-(4-(1-methyl-1*H*-imidazol-4-yl)phenoxy)propanamide (**31**). 4-(4-Bromophenyl)-1*H*-imidazol-2-amine **50** (48 mg, 0.20 mmol) was reacted with the acid chloride **60** (53 mg, 0.20 mmol) and Et₃N (112 μL, 0.80 mmol) according to general method C. The crude product was purified by flash chromatography (0–20% v/v MeOH in DCM) to give compound **31** as a white solid (64 mg, 0.14 mmol, 67% yield). ¹H NMR (500 MHz, CDCl₃) δ 10.79 (br s, 1H), 9.49 (br s, 1H), 7.69 (d, *J* = 8.7 Hz, 2H), 7.58–7.41 (m, 5H), 7.18–6.97 (m, 2H), 6.93 (d, *J* = 8.8 Hz, 2H), 4.86 (d, *J* = 6.8 Hz, 1H), 3.71 (s, 3H), 1.65 (d, *J* = 6.7 Hz, 3H) ppm. ¹³C NMR (125 MHz, CDCl₃) δ 171.5, 155.2, 141.8, 141.2, 138.0, 137.2, 131.7, 129.1, 127.6, 126.3, 120.5, 115.8, 115.6, 115.3, 108.1, 74.6, 33.5, 18.5 ppm. LCMS (ESI⁺) *m/z* 465.9 [M + H]⁺, retention time 2.73 min (95%). HRMS (ESI⁺): *m/z* calculated for C₂₂H₂₁BrN₅O₂ [M + H]⁺: 466.0879. Found: 466.0874. ((*S*)-**31**): 69% yield. [α]_D²⁵ -40.2 (c 1.0, CHCl₃). LCMS (ESI⁺) *m/z* 466.0 [M + H]⁺, retention time 2.70 min (95%). HRMS (ESI⁺): *m/z* calculated for C₂₂H₂₁BrN₅O₂ [M + H]⁺: 466.0879. Found: 466.0879.

N-(4-(1*H*-imidazol-4-yl)phenyl)-2-((4-phenyl-1*H*-imidazol-2-yl)-thio)acetamide (**32**). Compound **43** (40 mg, 0.17 mmol) was reacted with 4-(4-bromophenyl)-1*H*-imidazole-2-thiol (30 mg, 0.17 mmol) according to general method A. Purification by flash chromatography (1–20% v/v MeOH in DCM) afforded **32** (41 mg, 0.11 mmol, 65% yield) as a white solid. ¹H NMR (400 MHz, DMSO-*d*₆) δ 12.46 (br s, 2H), 10.42 (br s, 1H), 7.76 (br s, 2H), 7.68 (d, *J* = 8.2 Hz, 4H), 7.56 (d, *J* = 8.5 Hz, 2H), 7.52 (s, 1H), 7.34 (br s, 2H), 7.19 (br s, 1H), 3.99 (s, 2H) ppm. ¹³C NMR (125 MHz, DMSO-*d*₆) δ 167.0, 141.7, 139.9, 137.7, 136.2, 134.6, 128.9, 126.7, 125.2, 124.6, 119.7, 115.4, 39.5 ppm. LCMS (ESI⁺) *m/z* 376.1 [M + H]⁺, retention time 0.88 min (100%). HRMS (ESI⁺): *m/z* calculated for C₂₀H₁₈N₅OS [M + H]⁺: 376.1232. Found: 376.1241.

N-(4-(4-Bromophenyl)oxazol-2-yl)-2-(4-(1-methyl-1*H*-imidazol-4-yl)phenoxy)propanamide (**33**). 4-(4-Bromophenyl)oxazol-2-amine **61** (39 mg, 0.16 mmol) was reacted with the acid chloride **60** (43 mg, 0.16 mmol) and Et₃N (90 μL, 0.64 mmol) according to general method C. The crude product was purified by flash chromatography (0–15% v/v MeOH in DCM) to give compound **33** as a white solid (49 mg, 0.10 mmol, 64% yield). ¹H NMR (400 MHz, CDCl₃) δ 9.13 (br s, 1H), 7.81–7.66 (m, 3H), 7.63–7.50 (m, 4H), 7.47 (s, 1H), 7.13 (d, *J* = 1.3 Hz, 1H), 7.03–6.94 (m, 2H), 4.90 (q, *J* = 6.6 Hz, 1H), 3.74 (s, 3H), 1.70 (d, *J* = 6.8 Hz, 3H) ppm. ¹³C NMR (100 MHz, CDCl₃) δ 155.1, 141.7, 138.0, 131.9, 131.7, 130.3, 129.4, 129.3, 127.8, 127.0, 126.7, 126.4, 122.2, 116.0, 115.4, 75.1, 33.5, 18.4 ppm. LCMS (ESI⁺) *m/z* 468.9 [M + H]⁺, retention time 2.86 min (95%). HRMS (ESI⁺): *m/z* calculated for C₂₂H₂₀BrN₄O₃ [M + H]⁺: 467.0719. Found: 467.0711.

2-(4-(1-Methyl-1*H*-imidazol-4-yl)phenoxy)-*N*-phenylpropanamide (**34**). Aniline (28 μL, 0.30 mmol) was reacted with the acid chloride **60** (53 mg, 0.20 mmol) and Et₃N (112 μL, 0.80 mmol) according to general method D. The crude product was purified by flash chromatography (0–20% v/v MeOH in DCM) to give compound **34** as a white solid (48 mg, 0.14 mmol, 74% yield). ¹H NMR (400 MHz, CDCl₃) δ 8.25 (br s, 1H), 7.79–7.69 (m, 2H), 7.60–7.52 (m, 2H), 7.47

(d, *J* = 1.3 Hz, 1H), 7.35 (dd, *J* = 8.5, 7.3 Hz, 2H), 7.19–7.06 (m, 2H), 7.05–6.97 (m, 2H), 4.82 (q, *J* = 6.7 Hz, 1H), 3.73 (s, 3H), 1.69 (d, *J* = 6.8 Hz, 3H) ppm. ¹³C NMR (100 MHz, CDCl₃) δ 170.3, 155.6, 141.8, 137.9, 137.0, 129.0, 129.0, 126.3, 124.7, 120.0, 116.0, 115.3, 75.6, 33.5, 18.7 ppm. LCMS (ESI⁺) *m/z* 322.2 [M + H]⁺, retention time 1.86 min (97%). HRMS (ESI⁺): *m/z* calculated for C₁₉H₂₀N₃O₂ [M + H]⁺: 322.1556. Found: 322.1552.

N-(4-Iodophenyl)-2-(4-(1-methyl-1*H*-imidazol-4-yl)phenoxy)propanamide (**35**). 4-Iodoaniline (65 mg, 0.30 mmol) was reacted with the acid chloride **60** (53 mg, 0.20 mmol) and Et₃N (112 μL, 0.80 mmol) according to the general method D. The crude product was purified by flash chromatography (0–20% v/v MeOH in DCM) to give compound **35** as a pink solid (62 mg, 0.14 mmol, 68% yield). ¹H NMR (400 MHz, CDCl₃) δ 8.28 (br s, 1H), 7.77–7.69 (m, 2H), 7.69–7.57 (m, 2H), 7.47 (d, *J* = 1.4 Hz, 1H), 7.41–7.31 (m, 2H), 7.11 (d, *J* = 1.3 Hz, 1H), 7.03–6.91 (m, 2H), 4.80 (q, *J* = 6.7 Hz, 1H), 3.73 (s, 3H), 1.67 (d, *J* = 6.8 Hz, 3H) ppm. ¹³C NMR (100 MHz, CDCl₃) δ 170.4, 155.5, 141.7, 137.9, 136.9, 129.0, 126.3, 126.0, 121.8, 116.0, 115.3, 87.9, 75.6, 33.5, 18.6 ppm. LCMS (ESI⁺) *m/z* 448.2 [M + H]⁺, retention time 2.47 min (96%). HRMS (ESI⁺): *m/z* calculated for C₁₉H₁₉I₂N₃O₂ [M + H]⁺: 448.0522. Found: 448.0517.

2-(4-(1-Methyl-1*H*-imidazol-4-yl)phenoxy)-*N*-(4-phenyl-1*H*-imidazol-2-yl)propanamide (**36**). 4-Phenyl-1*H*-imidazol-2-amine **51** (33 mg, 0.20 mmol) was reacted with the acid chloride **60** (53 mg, 0.20 mmol) and Et₃N (112 μL, 0.80 mmol) according to general method C. The crude product was purified by flash chromatography (0–15% v/v MeOH in DCM) to give compound **36** as a brown solid (57 mg, 0.15 mmol, 72% yield). ¹H NMR (400 MHz, CDCl₃) δ 10.84 (br s, 1H), 9.51 (br s, 1H), 7.78–7.56 (m, 4H), 7.46 (d, *J* = 1.2 Hz, 1H), 7.39 (t, *J* = 7.7 Hz, 2H), 7.22–7.26 (m, 1H), 7.14 (s, 1H), 7.11 (d, *J* = 1.4 Hz, 1H), 7.02–6.89 (m, 2H), 4.89 (q, *J* = 6.8 Hz, 1H), 3.73 (s, 3H), 1.68 (d, *J* = 6.8 Hz, 3H) ppm. ¹³C NMR (125 MHz, CDCl₃) δ 171.3, 155.2, 141.8, 137.9, 129.1, 128.7, 126.9, 126.3, 124.6, 115.9, 115.3, 107.8, 74.5, 33.5, 18.5 ppm. LCMS (ESI⁺) *m/z* 388.1 [M + H]⁺, retention time 4.44 min (100%). HRMS (ESI⁺): *m/z* calculated for C₂₂H₂₂N₅O₂ [M + H]⁺: 388.1773. Found: 388.1767.

2-(4-(1-Methyl-1*H*-imidazol-4-yl)phenoxy)-*N*-(4-(4-morpholinophenyl)-1*H*-imidazol-2-yl)propanamide (**37**). 4-(4-Morpholinophenyl)-1*H*-imidazol-2-amine **52** (40 mg, 0.16 mmol) was reacted with the acid chloride **60** (43 mg, 0.16 mmol) and Et₃N (90 μL, 0.65 mmol) according to general method C. The crude product was purified by flash chromatography (3–15% v/v MeOH in DCM) to give compound **37** as a brown solid (51 mg, 0.11 mmol, 67% yield). ¹H NMR (400 MHz, CDCl₃) δ 10.74 (br s, 1H), 7.71 (d, *J* = 8.8 Hz, 2H), 7.54 (br s, 2H), 7.47 (d, *J* = 1.4 Hz, 1H), 7.11 (d, *J* = 1.4 Hz, 1H), 7.03–6.88 (m, 5H), 4.90 (q, *J* = 6.7 Hz, 1H), 4.06–3.83 (m, 4H), 3.73 (s, 3H), 3.27–3.01 (m, 4H), 1.69 (d, *J* = 6.8 Hz, 3H) ppm. ¹³C NMR (125 MHz, CDCl₃) δ 171.5, 155.3, 150.3, 141.8, 141.0, 137.9, 137.8, 128.9, 126.3, 125.5, 115.8, 115.3, 74.4, 66.9, 49.3, 33.6, 18.7 ppm. LCMS (ESI⁺) *m/z* 473.2 [M + H]⁺, retention time 2.22 min (100%). HRMS (ESI⁺): *m/z* calculated for C₂₆H₂₉N₆O₃ [M + H]⁺: 473.2301. Found: 473.2297.

N-(4-(4-Methoxyphenyl)-1*H*-imidazol-2-yl)-2-(4-(1-methyl-1*H*-imidazol-4-yl)phenoxy)propanamide (**38**). 4-(4-Methoxyphenyl)-1*H*-imidazol-2-amine **53** (30 mg, 0.16 mmol) was reacted with the acid chloride **60** (43 mg, 0.16 mmol) and Et₃N (90 μL, 0.65 mmol) according to general method C. The crude product was purified by flash chromatography (1–20% v/v MeOH in DCM) to give compound **38** as a yellow solid (45 mg, 0.11 mmol, 67% yield). ¹H NMR (400 MHz, CDCl₃) δ 10.73 (br s, 1H), 9.62 (br s, 1H), 7.78–7.65 (m, 2H), 7.57 (br s, 2H), 7.46 (d, *J* = 1.4 Hz, 1H), 7.10 (d, *J* = 1.3 Hz, 1H), 7.02 (s, 1H), 6.95 (dd, *J* = 10.5, 8.8 Hz, 4H), 4.88 (q, *J* = 6.8 Hz, 1H), 3.84 (s, 3H), 3.73 (s, 3H), 1.68 (d, *J* = 6.8 Hz, 3H) ppm. ¹³C NMR (125 MHz, CDCl₃) δ 171.4, 158.7, 155.3, 141.8, 140.8, 137.9, 129.1, 126.3, 125.8, 115.8, 115.3, 114.2, 74.7, 55.3, 33.4, 18.4 ppm. LCMS (ESI⁺) *m/z* 418.3 [M + H]⁺, retention time 4.69 min (100%). HRMS (ESI⁺): *m/z* calculated for C₂₃H₂₄N₅O₃ [M + H]⁺: 418.1879. Found: 418.1875.

N-(4-(4-Iodophenyl)-1*H*-imidazol-2-yl)-2-(4-(1-methyl-1*H*-imidazol-4-yl)phenoxy)propanamide (**39**). 4-(4-Iodophenyl)-1*H*-imidazol-2-amine **54** (46 mg, 0.16 mmol) was reacted with the acid chloride **60** (43 mg, 0.16 mmol) and Et₃N (90 μL, 0.65 mmol) according to general

method C. The crude product was purified by flash chromatography (1–20% v/v MeOH in DCM) to give compound **39** as a yellow solid (50 mg, 0.10 mmol, 61% yield). ^1H NMR (500 MHz, CDCl_3) δ 10.75 (br s, 1H), 9.42 (br s, 1H), 7.69 (t, $J = 8.3$ Hz, 4H), 7.53–7.33 (m, 3H), 7.10 (d, $J = 8.3$ Hz, 2H), 6.95 (d, $J = 8.9$ Hz, 2H), 4.88 (q, $J = 6.7$ Hz, 1H), 3.71 (s, 3H), 1.66 (d, $J = 6.7$ Hz, 3H) ppm. ^{13}C NMR (125 MHz, CDCl_3) δ 171.5, 155.2, 141.7, 138.0, 137.7, 129.1, 126.5, 126.3, 115.8, 115.3, 108.1, 91.8, 74.5, 33.5, 18.5 ppm. LCMS (ESI+) m/z 514.2 [M + H] $^+$, retention time 4.61 min (95%). HRMS (ESI+): m/z calculated for $\text{C}_{22}\text{H}_{21}\text{IN}_3\text{O}_2$ [M + H] $^+$: 514.0740. Found: 514.0740.

2-Chloro-N-phenylacetamide (40). Aniline (400 μL , 4.38 mmol) was reacted with chloroacetyl chloride (380 μL , 4.77 mmol) and Et_3N (670 μL , 4.77 mmol) according to general method E, and used in subsequent reactions without further purification. Compound **40** was obtained (720 mg, 4.24 mmol, 96% yield) as a green solid and was used without further purification. ^1H NMR (400 MHz, CDCl_3) δ 8.27 (br s, 1H), 7.58 (d, $J = 7.7$ Hz, 2H), 7.39 (t, $J = 7.9$ Hz, 2H), 7.20 (t, $J = 7.4$ Hz, 1H), 4.22 (s, 2H) ppm. ^{13}C NMR (100 MHz, CDCl_3) δ 163.9, 136.8, 129.3, 125.4, 120.2, 43.0 ppm. LCMS (ESI+) m/z 170.1 [M + H] $^+$, retention time 1.58 min (100%). HRMS (ESI+): m/z calculated for $\text{C}_8\text{H}_9\text{ClNO}$ [M + H] $^+$: 170.0373. Found: 170.0366. NMR data is in accordance with literature values.³⁹

N-(Benzofuran-5-yl)-2-chloroacetamide (41). Benzofuran-5-amine (140 mg, 1.05 mmol) was reacted with chloroacetyl chloride (93 μL , 1.16 mmol) and Et_3N (162 μL , 1.16 mmol) according to general method E, and it was used in subsequent reactions without further purification. Compound **41** was obtained (219 mg, 1.04 mmol, 99% yield) as a green solid and was used without further purification. ^1H NMR (400 MHz, CDCl_3) δ 8.41 (br s, 1H), 7.94 (d, $J = 2.2$ Hz, 1H), 7.64 (d, $J = 2.2$ Hz, 1H), 7.47 (dd, $J = 8.8, 0.8$ Hz, 1H), 7.32 (dd, $J = 8.8, 2.2$ Hz, 1H), 6.76 (dd, $J = 2.2, 0.9$ Hz, 1H), 4.23 (s, 2H) ppm. ^{13}C NMR (100 MHz, CDCl_3) δ 163.9, 152.4, 146.1, 131.9, 127.9, 117.7, 113.3, 111.6, 106.8, 43.0 ppm. LCMS (ESI+) m/z 210.1 [M + H] $^+$, retention time 1.71 min (100%). HRMS (ESI+): m/z calculated for $\text{C}_{11}\text{H}_9\text{ClNO}_2$ [M + H] $^+$: 210.0322. Found: 210.0319.

2-Chloro-N-(4-iodophenyl)acetamide (42). 4-Iodoaniline (500 mg, 2.28 mmol) was reacted with chloroacetyl chloride (200 μL , 2.51 mmol) and Et_3N (350 μL , 2.51 mmol) according to general method E. The crude product was purified by flash chromatography (10–100% v/v EtOAc in petroleum ether) to give compound **42** as a brown solid (600 mg, 2.03 mmol, 89% yield). ^1H NMR (400 MHz, CDCl_3) δ 8.32–8.11 (br s, 1H), 7.69 (d, $J = 8.8$ Hz, 2H), 7.36 (d, $J = 8.7$ Hz, 2H), 4.20 (s, 2H) ppm. ^{13}C NMR (100 MHz, CDCl_3) δ 163.8, 138.1, 136.4, 121.8, 88.7, 42.9 ppm. LCMS (ESI–) m/z 293.7 [M – H] $^-$, retention time 2.38 min (100%). HRMS (ESI–): m/z calculated for $\text{C}_8\text{H}_6\text{ClINO}$ [M – H] $^-$: 293.9183. Found: 293.9187. NMR data is in accordance with literature values.⁴⁰

N-(4-(1H-Imidazol-4-yl)phenyl)-2-chloroacetamide (43). 4-(1H-Imidazol-4-yl)aniline (200 mg, 1.25 mmol) was reacted with chloroacetyl chloride (109 μL , 1.38 mmol) and Et_3N (192 μL , 1.38 mmol) according to general method E. The crude product was purified by flash chromatography (3–20% v/v MeOH in DCM) to give compound **43** as a yellow solid (264 mg, 1.12 mmol, 89% yield). ^1H NMR (400 MHz, $\text{DMSO}-d_6$) δ 10.43 (br s, 1H), 9.83 (br s, 1H), 7.98 (br s, 1H), 7.77–7.65 (m, 2H), 7.70–7.47 (m, 3H), 4.27 (s, 2H) ppm. LCMS (ESI+) m/z 236.2 [M + H] $^+$, retention time 1.15 min (100%). HRMS (ESI+): m/z calculated for $\text{C}_{11}\text{H}_{10}\text{ClN}_3\text{O}$ [M + H] $^+$: 236.0591. Found: 236.0590.

(5-(4-Bromophenyl)-1H-imidazol-2-yl)methanamine Hydrochloride (44). 4 M HCl (2 mL) was added slowly to a stirred solution of benzyl ((5-(4-bromophenyl)-1H-imidazol-2-yl)methyl)carbamate³⁶ (105 mg, 0.26 mmol) in dioxane (1 mL). The mixture was stirred at 100 $^\circ\text{C}$ for 4 h, and then the solvents were removed under reduced pressure to give the desired product as a white solid (86 mg, 0.26 mmol, 100% yield). ^1H NMR (500 MHz, MeOD) δ 8.00 (s, 1H), 7.75–7.67 (m, 4H), 4.55 (s, 2H) ppm. ^{13}C NMR (125 MHz, MeOD) δ 140.8, 136.0, 133.7, 128.4, 127.6, 124.7, 117.8, 111.4, 34.8 ppm. LCMS (ESI–) m/z 250.1 [M – H] $^-$, retention time 2.13 min (100%). HRMS (ESI–): m/z calculated for $\text{C}_{10}\text{H}_9\text{BrN}_3$ [M + H] $^+$: 249.9980. Found: 249.9987.

N-(4-(4-Bromophenyl)-1H-imidazol-2-yl)acetamide (45). Following general method F, from 2-bromo-1-(4-bromophenyl)ethanone (104 mg, 0.38 mmol) was obtained **45** (88 mg, 0.31 mmol, 84% yield) as a green solid. ^1H NMR (500 MHz, $\text{DMSO}-d_6$) δ 11.66 (br s, 1H), 11.20 (br s, 1H), 7.72–7.57 (m, 2H), 7.54–7.42 (m, 2H), 7.30 (d, $J = 1.6$ Hz, 1H), 2.05 (s, 3H) ppm. ^{13}C NMR (125 MHz, $\text{DMSO}-d_6$) δ 169.0, 141.9, 135.5, 134.4, 131.7, 126.4, 119.0, 110.4, 23.3 ppm. LCMS (ESI+) m/z 282.1 [M + H] $^+$, retention time 2.13 min (100%). HRMS (ESI+): m/z calculated for $\text{C}_{11}\text{H}_{11}\text{BrN}_3\text{O}$ [M + H] $^+$: 280.0085. Found: 280.0080. NMR data is in accordance with literature values.³⁷

N-(4-Phenyl-1H-imidazol-2-yl)acetamide (46). Following general method F, from 2-bromo-1-phenylethan-1-one (100 mg, 0.50 mmol) was obtained **46** (79 mg, 0.39 mmol, 78% yield) as a green solid. ^1H NMR (400 MHz, $\text{DMSO}-d_6$) δ 11.59 (br s, 1H), 11.24 (br s, 1H), 7.71 (d, $J = 7.6$ Hz, 2H), 7.32 (t, $J = 7.6$ Hz, 2H), 7.25 (br s, 1H), 7.16 (t, $J = 7.4$ Hz, 1H), 2.07 (s, 3H) ppm. ^{13}C NMR (100 MHz, $\text{DMSO}-d_6$) δ 169.0, 141.7, 136.6, 128.9, 126.3, 124.4, 109.6, 23.3 ppm. LCMS (ESI–) m/z 200.0 [M – H] $^-$, retention time 1.44 min (100%). HRMS (ESI+): m/z calculated for $\text{C}_{11}\text{H}_{12}\text{N}_3\text{O}$ [M + H] $^+$: 202.0980. Found: 202.0977. NMR data is in accordance with literature values.³⁷

N-(4-(4-Morpholinophenyl)-1H-imidazol-2-yl)acetamide (47). Following general method F, from 2-bromo-1-(4-(piperidin-1-yl)phenyl)ethan-1-one (106 mg, 0.38 mmol) was obtained **47** (90 mg, 0.31 mmol, 83% yield) as a brown solid. ^1H NMR (500 MHz, $\text{DMSO}-d_6$) δ 11.46 (br s, 1H), 11.17 (br s, 1H), 7.55 (d, $J = 8.2$ Hz, 2H), 7.06 (br s, 1H), 6.89 (d, $J = 8.5$ Hz, 2H), 3.93–3.53 (m, 4H), 3.07 (t, $J = 4.8$ Hz, 4H), 2.04 (s, 3H) ppm. ^{13}C NMR (125 MHz, $\text{DMSO}-d_6$) δ 168.8, 149.8, 141.4, 136.8, 125.2, 115.6, 113.5, 107.9, 66.6, 49.0, 23.2 ppm. LCMS (ESI–) m/z 285.1 [M – H] $^-$, retention time 1.60 min (95%). HRMS (ESI+): m/z calculated for $\text{C}_{15}\text{H}_{19}\text{N}_4\text{O}_2$ [M + H] $^+$: 287.1508. Found: 287.1505.

N-(4-(4-Methoxyphenyl)-1H-imidazol-2-yl)acetamide (48). Following general method F, from 2-bromo-1-(4-methoxyphenyl)ethan-1-one (150 mg, 0.66 mmol) was obtained **48** (110 mg, 0.47 mmol, 71% yield) as a white solid. ^1H NMR (400 MHz, $\text{DMSO}-d_6$) δ 11.52 (br s, 1H), 11.20 (br s, 1H), 7.62 (d, $J = 8.1$ Hz, 2H), 7.11 (s, 1H), 6.89 (d, $J = 8.4$ Hz, 2H), 3.75 (s, 3H), 2.06 (s, 3H) ppm. ^{13}C NMR (100 MHz, $\text{DMSO}-d_6$) δ 168.5, 157.8, 141.2, 136.1, 127.6, 125.3, 113.9, 107.9, 55.1, 22.9 ppm. LCMS (ESI–) m/z 230.1 [M – H] $^-$, retention time 1.52 min (96%). HRMS (ESI+): m/z calculated for $\text{C}_{12}\text{H}_{14}\text{N}_3\text{O}_2$ [M + H] $^+$: 232.1086. Found: 232.1082. NMR data is in accordance with literature values.³⁷

N-(4-(4-Iodophenyl)-1H-imidazol-2-yl)acetamide (49). Following general method F, from 2-bromo-1-(4-iodophenyl)ethan-1-one (214 mg, 0.66 mmol) was obtained **49** (190 mg, 0.58 mmol, 88% yield) as a green solid. ^1H NMR (500 MHz, $\text{DMSO}-d_6$) δ 11.66 (br s, 1H), 11.21 (br s, 1H), 7.64 (d, $J = 8.1$ Hz, 2H), 7.51 (d, $J = 8.1$ Hz, 2H), 7.30 (s, 1H), 2.05 (s, 3H) ppm. ^{13}C NMR (125 MHz, $\text{DMSO}-d_6$) δ 168.5, 141.4, 137.1, 135.1, 134.3, 126.2, 109.9, 90.9, 22.8 ppm. LCMS (ESI–) m/z 326.0 [M – H] $^-$, retention time 2.43 min (100%). HRMS (ESI+): m/z calculated for $\text{C}_{11}\text{H}_{11}\text{IN}_3\text{O}$ [M + H] $^+$: 327.9947. Found: 327.9945.

4-(4-Bromophenyl)-1H-imidazol-2-amine (50). Following general method G, from *N*-(4-(4-bromophenyl)-1H-imidazol-2-yl)acetamide **45** (88 mg, 0.31 mmol) was obtained **50** (70 mg, 0.29 mmol, 95% yield) as a brown solid. ^1H NMR (500 MHz, $\text{DMSO}-d_6$) δ 7.52 (d, $J = 8.1$ Hz, 2H), 7.42 (d, $J = 8.6$ Hz, 2H), 7.04 (s, 1H), 5.40 (br s, 2H) ppm. ^{13}C NMR (125 MHz, $\text{DMSO}-d_6$) δ 150.4, 134.0, 131.2, 126.0, 125.4, 117.5, 110.5 ppm. LCMS (ESI+) m/z 240.1 [M + H] $^+$, retention time 1.50 min (97%). HRMS (ESI+): m/z calculated for $\text{C}_9\text{H}_9\text{BrN}_3$ [M + H] $^+$: 237.9980. Found: 237.9980. NMR data is in accordance with literature values.³⁷

4-Phenyl-1H-imidazol-2-amine (51). Following general method G, from *N*-(4-phenyl-1H-imidazol-2-yl)acetamide **46** (70 mg, 0.35 mmol) was obtained **51** (47 mg, 0.29 mmol, 84% yield) as a red solid. ^1H NMR (400 MHz, MeOD) δ 7.62–7.46 (m, 2H), 7.31 (t, $J = 7.7$ Hz, 2H), 7.16 (td, $J = 7.5, 1.2$ Hz, 1H), 6.91 (s, 1H) ppm. ^{13}C NMR (125 MHz, MeOD) δ 150.3, 132.9, 128.4, 128.1, 125.6, 123.5, 111.2 ppm. LCMS (ESI+) m/z 160.1 [M + H] $^+$, retention time 1.45 min (100%). HRMS (ESI+): m/z calculated for $\text{C}_9\text{H}_{10}\text{BrN}_3$ [M + H] $^+$: 160.0875. Found: 160.0873. NMR data is in accordance with literature values.³⁷

4-(4-Morpholinophenyl)-1H-imidazol-2-amine (52). Following general method G, from *N*-(4-(4-morpholinophenyl)-1H-imidazol-2-yl)acetamide **47** (85 mg, 0.30 mmol) was obtained **52** (60 mg, 0.24 mmol, 82% yield) as a brown solid. ¹H NMR (400 MHz, MeOD) δ 7.47 (d, *J* = 8.8 Hz, 2H), 6.96 (d, *J* = 8.8 Hz, 2H), 6.78 (s, 1H), 3.91–3.64 (m, 4H), 3.19–3.02 (m, 4H) ppm. ¹³C NMR (125 MHz, MeOD) δ 149.9, 149.8, 129.3, 125.0, 124.5, 115.8, 113.0, 66.6, 49.4 ppm. LCMS (ESI+) *m/z* 245.1 [M + H]⁺, retention time 1.50 min (100%). HRMS (ESI+): *m/z* calculated for C₁₃H₁₇N₄O [M + H]⁺: 245.1402. Found: 245.1390.

4-(4-Methoxyphenyl)-1H-imidazol-2-amine (53). Following general method G, from *N*-(4-(4-methoxyphenyl)-1H-imidazol-2-yl)acetamide **48** (83 mg, 0.36 mmol) was obtained **53** (65 mg, 0.34 mmol, 95% yield) as a brown solid. ¹H NMR (400 MHz, MeOD) δ 7.54–7.39 (m, 2H), 7.04–6.85 (m, 2H), 6.78 (s, 1H), 3.81 (s, 3H) ppm. ¹³C NMR (100 MHz, MeOD) δ 158.3, 150.0, 125.9, 125.0, 124.8, 113.6, 109.8, 54.3 ppm. LCMS (ESI+) *m/z* 190.2 [M + H]⁺, retention time 1.61 min (100%). HRMS (ESI+): *m/z* calculated for C₁₀H₁₂N₃O [M + H]⁺: 190.0980. Found: 190.0979. NMR data is in accordance with literature values.³⁷

4-(4-Iodophenyl)-1H-imidazol-2-amine (54). Following general method G, from *N*-(4-(4-iodophenyl)-1H-imidazol-2-yl)acetamide **49** (150 mg, 0.46 mmol) was obtained **54** (103 mg, 0.36 mmol, 79% yield) as a red solid. ¹H NMR (500 MHz, DMSO-*d*₆) δ 7.58 (d, *J* = 8.3 Hz, 2H), 7.38 (d, *J* = 8.2 Hz, 2H), 7.03 (s, 1H), 5.35 (br s, 2H) ppm. ¹³C NMR (125 MHz, DMSO-*d*₆) δ 150.8, 137.4, 134.6, 133.4, 126.0, 111.1, 90.2 ppm. LCMS (ESI+) *m/z* 286.1 [M + H]⁺, retention time 2.09 min (100%). HRMS (ESI+): *m/z* calculated for C₉H₉IN₃ [M + H]⁺: 285.9841. Found: 285.9846.

4-(1H-imidazol-4-yl)phenol (55). 2-Bromo-1-(4-hydroxyphenyl)ethan-1-one (1.0 g, 4.67 mmol) was dissolved in formamide (5 mL), and the reaction mixture was heated at 150 °C for 24 h. After cooling to rt, the resulting mixture was diluted with EtOAc (40 mL) and washed with saturated aqueous NaHCO₃ (40 mL). The aqueous layer was extracted with EtOAc (2 × 40 mL), and the combined organic layers were dried over MgSO₄, filtered, and concentrated to give **55** (0.75 g, 4.67 mmol, 99% yield) as a brown oil. ¹H NMR (400 MHz, MeOD) δ 8.17 (br s, 1H), 7.68 (d, *J* = 1.2 Hz, 1H), 7.64–7.44 (m, 2H), 7.25 (d, *J* = 1.1 Hz, 1H), 6.82 (d, *J* = 8.6 Hz, 2H) ppm. ¹³C NMR (100 MHz, MeOD) δ 156.3, 135.1, 125.8, 124.3, 115.1 ppm. LCMS (ESI+) *m/z* 161.2 [M + H]⁺, retention time 0.54 min (100%). HRMS (ESI+): *m/z* calculated for C₉H₉N₂O [M + H]⁺: 161.0715. Found: 161.0720. NMR data is in accordance with literature values.³⁸

4-(4-Methoxyphenyl)-1-methyl-1H-imidazole (56). To a solution of **55** (2.77 g, 17 mmol) in DMF (20 mL) containing cesium carbonate (12.4 g, 38 mmol) at rt was added iodomethane (2.4 mL, 38 mmol). The reaction mixture was stirred at rt for 8 h. The reaction mixture was then cooled to 0 °C and quenched with H₂O (70 mL) and extracted with EtOAc (3 × 60 mL). The combined organic layers were washed with brine (3 × 100 mL), dried over MgSO₄, filtered, and concentrated to give **56** (2.8 g, 15 mmol, 88% yield) as a brown solid. ¹H NMR (400 MHz, CDCl₃) δ 7.71 (d, *J* = 8.8 Hz, 2H), 7.46 (d, *J* = 1.3 Hz, 1H), 7.10 (d, *J* = 1.4 Hz, 1H), 6.94 (d, *J* = 8.9 Hz, 2H), 3.85 (s, 3H), 3.73 (s, 3H) ppm. ¹³C NMR (100 MHz, CDCl₃) δ 158.6, 142.4, 137.8, 127.2, 126.0, 114.8, 114.0, 55.3, 33.5. LCMS (ESI+) *m/z* 189.2 [M + H]⁺, retention time 1.38 min (100%). HRMS (ESI+): *m/z* calculated for C₁₁H₁₃N₂O [M + H]⁺: 189.1028. Found: 189.1031. NMR data is in accordance with literature values.⁴¹

4-(1-Methyl-1H-imidazol-4-yl)phenol (57). A solution of 4-(4-methoxyphenyl)-1-methyl-1H-imidazole **56** (1.21 g, 6.42 mmol) in anhydrous DCM (30 mL) at –78 °C was treated with BBr₃ (16 mL, 16.05 mmol, 1 M in DCM). The reaction mixture was stirred at –78 °C for 10 min and 2 h at rt. The reaction mixture was then cooled to –78 °C and quenched with MeOH (4 mL). The solvents were then removed under reduced pressure, and the crude product was redissolved in EtOAc (50 mL) and washed with saturated NaHCO₃ solution. The aqueous phase was extracted with EtOAc (2 × 50 mL), and the combined organic fractions were dried with anhydrous MgSO₄ and filtered off, and the solvent was removed under vacuum to give **57** (1.30 g, 6.17 mmol, 96% yield) as a brown solid, which was used in the next step without further purification. ¹H NMR (400 MHz, MeOD) δ 8.99–

8.80 (m, 1H), 7.77 (d, *J* = 1.6 Hz, 1H), 7.55 (d, *J* = 8.7 Hz, 2H), 6.93 (d, *J* = 8.8 Hz, 2H), 3.99 (s, 3H) ppm. ¹³C NMR (100 MHz, MeOD) δ 159.1, 135.1, 134.6, 126.9, 117.3, 117.2, 115.8, 35.0 ppm. LCMS (ESI+) *m/z* 175.1 [M + H]⁺, retention time 1.09 min (100%). HRMS (ESI+): *m/z* calculated for C₁₀H₁₁N₂O [M + H]⁺: 175.0871. Found: 175.0870.

Methyl 2-(4-(1-Methyl-1H-imidazol-4-yl)phenoxy)propanoate (58). Cs₂CO₃ (3.46 g, 10.62 mmol) and methyl 2-bromopropanoate (1.29 g, 6.81 mmol) were added to a solution of phenol derivative **57** (1.12 g, 5.32 mmol) in anhydrous DMF (10 mL), and the mixture was stirred at rt for 1 h and at 60 °C for 5 h. After cooling to rt, the reaction was diluted with water (80 mL) and extracted with EtOAc (2 × 80 mL). The combined organic layers were washed with brine (3 × 100 mL), dried over MgSO₄, filtered, and concentrated. The crude product was purified by flash chromatography (0–20% v/v MeOH in DCM) to give **58** (1.30 g, 4.99 mmol, 92% yield) as an orange oil. ¹H NMR (400 MHz, CDCl₃) δ 7.74–7.61 (m, 2H), 7.45 (d, *J* = 1.3 Hz, 1H), 7.08 (d, *J* = 1.4 Hz, 1H), 6.96–6.81 (m, 2H), 4.81 (q, *J* = 6.8 Hz, 1H), 3.77 (s, 3H), 3.71 (s, 3H), 1.64 (d, *J* = 6.8 Hz, 3H) ppm. ¹³C NMR (100 MHz, CDCl₃) δ 172.8, 156.5, 142.1, 137.8, 128.1, 126.0, 115.3, 115.1, 72.7, 52.3, 33.5, 18.6 ppm. LCMS (ESI+) *m/z* 261.3 [M + H]⁺, retention time 1.50 min (100%). HRMS (ESI+): *m/z* calculated for C₁₄H₁₇N₂O₃ [M + H]⁺: 261.1239. Found: 261.1232.

2-(4-(1-Methyl-1H-imidazol-4-yl)phenoxy)propanoic Acid (59). Methyl 2-(4-(1-methyl-1H-imidazol-4-yl)phenoxy)propanoate **58** (0.53 g, 2.04 mmol) was dissolved in a 2:1 v/v mixture of THF and H₂O (7.5 mL), and then NaOH (0.16 g, 4.08 mmol) was added. The reaction mixture was heated at 80 °C for 40 min. After the reaction mixture was allowed to cool to rt, the solvents were removed. The mixture was then diluted with H₂O (5 mL) and acidified to pH 7–8 using 1 N HCl. The mixture was cooled, and the resulting precipitate was collected by filtration, washed with water (2 × 3 mL) and petroleum ether (2 × 3 mL), and dried *in vacuo* to afford acid **59** (0.33 g, 1.33 mmol, 65% yield) as a white solid. ¹H NMR (400 MHz, DMSO-*d*₆) δ 7.69–7.55 (m, 3H), 7.46 (d, *J* = 1.3 Hz, 1H), 6.84 (d, *J* = 8.8 Hz, 2H), 4.81 (q, *J* = 6.8 Hz, 1H), 3.66 (s, 3H), 1.49 (d, *J* = 6.7 Hz, 3H). ¹³C NMR (100 MHz, DMSO-*d*₆) δ 173.3, 156.1, 140.4, 138.2, 127.8, 125.4, 115.8, 114.8, 71.7, 33.1, 18.4. LCMS (ESI+) *m/z* 247.2 [M + H]⁺, retention time 1.43 min (100%). HRMS (ESI+): *m/z* calculated for C₁₃H₁₅N₂O₃ [M + H]⁺: 247.1083. Found: 247.1080.

(S)-2-(4-(1-Methyl-1H-imidazol-4-yl)phenoxy)propanoic Acid ((S)-59). To a solution of **57** (212 mg, 1.21 mmol) in anhydrous THF (5 mL) was added ethyl D-lactate (215 mg, 1.82 mmol). After the reaction mixture was cooled to 0 °C, PPh₃ (478 mg, 1.82 mmol) and DEAD (286 μL, 1.82 mmol) were added, and the reaction mixture was stirred for 16 h at rt. The reaction mixture was poured into ice–water (40 mL) and extracted with DCM (3 × 50 mL). The combined organic layers were washed with brine, dried over anhydrous MgSO₄, filtered, and concentrated. The crude product was purified by flash chromatography (0–15% v/v MeOH in DCM) to give ethyl (S)-2-(4-(1-methyl-1H-imidazol-4-yl)phenoxy)propanoate as an orange solid. LCMS (ESI+) *m/z* 275.3 [M + H]⁺, retention time 2.06 min (94%). Ethyl (S)-2-(4-(1-methyl-1H-imidazol-4-yl)phenoxy)propanoate (200 mg, 0.73 mmol) was dissolved in a 2:1 v/v mixture of THF and H₂O (7.5 mL), and then NaOH (58 mg, 1.46 mmol) was added. The reaction mixture was stirred at rt for 3 h, and the solvents were removed. The residue was dissolved in EtOAc (40 mL) and then extracted with H₂O (40 mL). The aqueous layer was acidified to pH 7–8 using 1 N HCl. The mixture was cooled, and the resulting precipitate was collected by filtration, washed with water (2 × 3 mL) and petroleum ether (2 × 3 mL), and dried *in vacuo* to afford acid (S)-**59** (100 mg, 0.40 mmol, 56% yield) as a white solid. [α]_D²⁵ –51.6 (c 1.0, CHCl₃). LCMS (ESI+) *m/z* 247.2 [M + H]⁺, retention time 1.43 min (100%). HRMS (ESI+): *m/z* calculated for C₁₃H₁₅N₂O₃ [M + H]⁺: 247.1083. Found: 247.1079.

4-(4-Bromophenyl)oxazol-2-amine (61). A mixture of 2-bromo-1-(4-bromophenyl)ethanone (200 mg, 0.72 mmol) and urea (435 mg, 7.2 mmol) in anhydrous acetonitrile (5 mL) was heated at 80 °C for 18 h. The solvent was removed, and the residue was purified by flash chromatography (0–10% v/v MeOH in DCM) to afford **61** (134 mg, 0.56 mmol, 78% yield) as a yellow solid. ¹H NMR (400 MHz, MeOD) δ 7.68 (s, 1H), 7.59–7.42 (m, 4H) ppm. ¹³C NMR (125 MHz, MeOD) δ

163.9, 139.8, 132.7, 132.1, 128.8, 127.9, 122.1 ppm. LCMS (ESI+) m/z 238.8 $[M + H]^+$, retention time 1.95 min (100%). HRMS (ESI+): m/z calculated for $C_9H_8BrN_2O$ $[M + H]^+$: 238.9820. Found: 238.9816.

2. Enzyme Assay. The activity of *Mth* IMPDH Δ CBS was determined using a plate reader by monitoring the production of NADH in absorbance at 340 nm and corrected for noncatalyzed chemical reactions in the absence of *Mth* IMPDH Δ CBS. All the measurements were done in the assay buffer (50 mM Tris HCl pH 8, 1 mM DTT, 1 mM EDTA, and 100 mM KCl) at 37 °C with 20 nM *Mth* IMPDH Δ CBS, 2.8 mM NAD^+ , and 1 mM IMP in a total of 150 μ L volume in a 96 well plate-based format, and data were collected for 32 min. The reaction was initiated by the addition of the substrate, IMP, at a concentration of 1 mM. All reactions were performed in triplicate. Prior to reaction initiation, the compounds were preincubated in a buffer with enzyme for 5 min. The inhibitors were dissolved in DMSO- d_6 and diluted to a final concentration of 1% v/v in experimental reactions.

IC_{50} values were calculated by plotting the percentage of inhibition against the logarithm of inhibitor concentration, and dose–response curves were fitted using Prism software (GraphPad).

The K_i value for NAD^+ was determined at a constant saturating IMP concentration (1 mM) and five different concentrations of NAD^+ (0.35, 0.70, 1.0, 1.4, and 2.8 mM) in the presence of increasing concentrations of inhibitor. The value of K_i for IMP was determined at fixed saturating concentration of NAD^+ (2.8 mM) and different concentrations of IMP (0.12, 0.18, 0.25, 0.5, and 1 mM) and inhibitor.

The initial velocities at various inhibitor concentrations were determined based on the slope in the linear part of each reaction containing the inhibitor and the uninhibited reaction. To determine the inhibition constant (K_i values), the initial rate data versus substrate concentration at different inhibitor concentrations were fit using Prism software (GraphPad) to equations for uncompetitive or mixed inhibition. For each inhibitor concentration, the reciprocal of enzyme reaction velocity versus the reciprocal of the substrate concentration was plotted in a Lineweaver–Burk plot to determine the pattern of inhibition.

3. Protein Purification, Crystallization, and Data Collection of *Mth* IMPDH Δ CBS. *Mth* IMPDH was expressed, purified, and crystallized as previously described.^{24,25} Briefly, hexahistidine tagged *Mth* IMPDH Δ CBS in pHat2 was expressed overnight in BL21 DE3 (NEB) cells at 18 °C by addition of 500 μ M IPTG. Cells were lysed in 50 mM Hepes, pH 8.0, 500 mM NaCl, 5% glycerol, 10 mM β -mercaptoethanol, and 20 mM imidazole, and the recombinant protein purified using a Hi-Trap IMAC FF column (GE Healthcare) charged with nickel and an elution gradient of up to 300 mM imidazole. The hexahistidine tag was cleaved by TEV protease, and the purified *Mth* IMPDH Δ CBS was obtained by negative nickel gravity-flow purification⁴² and size exclusion chromatography on a Superdex 200 gel filtration column equilibrated in 20 mM Hepes pH 8.0, 500 mM NaCl, 5% glycerol, and 1 mM TCEP step. The recombinant *Mth* IMPDH Δ CBS was then concentrated to 12.5 mg/mL for crystallization.

Mth IMPDH Δ CBS protein crystallized in 1 μ L + 1 μ L hanging drops with 100 mM sodium acetate, pH 5.5, 200 mM calcium chloride, and 8–14% isopropanol. Crystals were soaked overnight in drops of well solution + 5 mM IMP and either 5 mM Fragment 2 or Compound 1 or 1 mM Compound 31. Crystals were cryoprotected by passing through drops containing well solution + 25% glycerol and flash-frozen in liquid nitrogen. Data were collected from the crystals at Diamond Light Source beamline.

4. Structure Solution, Ligand Fitting, and Refinement. Data were processed using XDS⁴³ and Pointless (CCP4). To solve the structure, molecular replacement was performed with Phenix Phaser⁴⁴ using a previously solved IMP-bound *Mth* IMPDH Δ CBS structure as a probe (PDB IDs: 5JSR; 5K4X; 5K4Z). Refinement was performed using Phenix.refine and manually in Coot.⁴⁵ IMP and the inhibitors were sequentially fitted into the density using the LigandFit function of Phenix, and the structures were manually refined further using Coot. Information regarding the crystallographic statistics can be found in Table S2. Protein–ligand interactions were analyzed using Arpeggio⁴⁶

and CSM-Lig.^{47,48} Compound properties were evaluated using pkCSM.⁴⁹ All figures made using Pymol (Schrodinger).

5. Drug Susceptibility Testing against *Mtb*. An Alamar Blue fluorescence-based broth microdilution assay was used to assess the minimum inhibitory concentration (MIC) of compounds against *Mtb* H37Rv, as described previously.^{25,50} Briefly, *Mtb* H37Rv was grown in standard Middlebrook 7H9 broth (BD) supplemented with OADC (BD), 0.2% glycerol, and 0.05% Tween-80 to midexponential phase. Compounds dissolved in DMSO (1%) were tested in clear-bottomed, round-well 96-well microtiter plates at eight different concentrations using the standard anti-TB drugs, rifampin and isoniazid, as positive controls. An inoculum of $\sim 10^5$ bacteria was added to each well, and the plates were incubated at 37 °C for 7 d. On day 7, 10 μ L of Alamar Blue (Invitrogen) was added to each well, and plates were further incubated at 37 °C for 24 h. The fluorescence (excitation 544 nm; emission 590 nm) was measured in a FLUOstar OPTIMA plate reader (BMG LABTECH, Offenberg, Germany). Data were normalized to the minimum and maximum inhibition controls to generate a dose response curve (% inhibition) from which the MIC_{90} was determined.

■ ASSOCIATED CONTENT

Supporting Information

The Supporting Information is available free of charge on the ACS Publications website at DOI: 10.1021/acs.jmedchem.7b01622.

¹H, ¹³C, and 2D NMR spectra of all new compounds, supplementary Figures S1–S2, whole-cell activity of compounds against *M. tuberculosis* H37Rv (Table S1), and X-ray data collection and refinement statistics (Table S2) (PDF)

Molecular formula strings data file for all chemical structures mentioned in the manuscript (CSV)

■ AUTHOR INFORMATION

Corresponding Authors

*T.L.B. email: tom@cryst.bioc.cam.ac.uk.

*D.B.A. phone, +61 3903 54794; e-mail, david.ascher@unimelb.edu.au.

*C.A. phone, +44 (0) 1223 336405; e-mail, ca26@cam.ac.uk.

ORCID

Ana Trapero: 0000-0003-4526-7895

Anthony G. Coyne: 0000-0003-0205-5630

Valerie Mizrahi: 0000-0003-4824-9115

Chris Abell: 0000-0001-9174-1987

Present Address

[#](V.S.) H3D Drug Discovery and Development Centre, Department of Chemistry and Institute of Infectious Disease and Molecular Medicine, University of Cape Town, Rondebosch 7701, Cape Town, South Africa.

Notes

The authors declare no competing financial interest.

Additional data related to this publication is available at the University of Cambridge data repository: <https://doi.org/10.17863/CAM.20512>. Structures have been deposited in the Protein Data Bank (PDB codes 5OU1 for IMPDH:IMP:Compound 1; 5OU2 for IMPDH:IMP:Compound 2 and 5OU3 for IMPDH:IMP:Compound 31 complex structures). Authors will release the atomic coordinates and experimental data upon article publication.

■ ACKNOWLEDGMENTS

This work was supported by the Bill and Melinda Gates Foundation (Hit-TB) and FP7 European Project MM4TB Grant

no. 260872. D.B.A was supported by a C. J. Martin Research Fellowship from the National Health and Medical Research Council of Australia (APP1072476) and the Jack Brockhoff Foundation (JBF 4186, 2016). D.B.A. and T.L.B. were also funded by a Newton Fund RCUK-CONFAP Grant awarded by The Medical Research Council and Fundação de Amparo à Pesquisa do Estado de Minas Gerais (MR/M026302/1). V.M. and V.S. were also supported by grants from the HHMI (Senior International Research Scholars grant to V.M.), the South African Medical Research Council, and the National Research Foundation.

■ ABBREVIATIONS USED

TB, tuberculosis; *Mycobacterium tuberculosis*, *Mtb*; MDR, multidrug resistant; XDR, extensively drug resistant; IMPDH, inosine-5'-monophosphate dehydrogenase; IMP, inosine 5'-monophosphate; CBS, cystathionine β -synthase; XMP, xanthosine monophosphate; NAD⁺, nicotinamide adenine dinucleotide; *Mth*, *Mycobacterium thermoresistibile*; MIC, minimal inhibitory concentration.; WHO, World Health Organization

■ REFERENCES

- (1) WHO. *Tuberculosis: Fact sheet*; World Health Organization 2016: Geneva, Switzerland. 2016.
- (2) Onyebujoh, P.; Zumla, A.; Ribeiro, I.; Rustomjee, R.; Mwaba, P.; Gomes, M.; Grange, J. M. Treatment of tuberculosis: present status and future prospects. *Bull. World Health Organ.* **2005**, *83*, 857–865.
- (3) Orenstein, E. W.; Basu, S.; Shah, N. S.; Andrews, J. R.; Friedland, G. H.; Moll, A. P.; Gandhi, N. R.; Galvani, A. P. Treatment outcomes among patients with multidrug-resistant tuberculosis: systematic review and meta-analysis. *Lancet Infect. Dis.* **2009**, *9*, 153–161.
- (4) Ratcliffe, A. J. Inosine 5'-monophosphate dehydrogenase inhibitors for the treatment of autoimmune diseases. *Curr. Opin. Drug Discovery Dev.* **2006**, *9*, 595–605.
- (5) Chen, L.; Pankiewicz, K. W. Recent development of IMP dehydrogenase inhibitors for the treatment of cancer. *Curr. Opin. Drug Discovery Dev.* **2007**, *10*, 403–412.
- (6) Olah, E.; Kokeny, S.; Papp, J.; Bozsik, A.; Keszei, M. Modulation of cancer pathways by inhibitors of guanylate metabolism. *Adv. Enzyme Regul.* **2006**, *46*, 176–190.
- (7) Nair, V.; Shu, Q. Inosine monophosphate dehydrogenase as a probe in antiviral drug discovery. *Antiviral Chem. Chemother.* **2007**, *18*, 245–258.
- (8) Shu, Q.; Nair, V. Inosine monophosphate dehydrogenase (IMPDH) as a target in drug discovery. *Med. Res. Rev.* **2008**, *28*, 219–232.
- (9) Shah, C. P.; Kharkar, P. S. Inosine 5'-monophosphate dehydrogenase inhibitors as antimicrobial agents: recent progress and future perspectives. *Future Med. Chem.* **2015**, *7*, 1415–1429.
- (10) Hedstrom, L.; Liechti, G.; Goldberg, J. B.; Gollapalli, D. R. The antibiotic potential of prokaryotic IMP dehydrogenase inhibitors. *Curr. Med. Chem.* **2011**, *18*, 1909–1918.
- (11) Hedstrom, L. IMP dehydrogenase: structure, mechanism, and inhibition. *Chem. Rev.* **2009**, *109*, 2903–2928.
- (12) Jackson, R. C.; Weber, G.; Morris, H. P. IMP dehydrogenase, an enzyme linked with proliferation and malignancy. *Nature* **1975**, *256*, 331–333.
- (13) Gilbert, H. J.; Lowe, C. R.; Drabble, W. T. Inosine 5'-monophosphate dehydrogenase of *Escherichia coli*. Purification by affinity chromatography, subunit structure and inhibition by guanosine 5'-monophosphate. *Biochem. J.* **1979**, *183*, 481–494.
- (14) Lee, S. A.; Gallagher, L. A.; Thongdee, M.; Staudinger, B. J.; Lippman, S.; Singh, P. K.; Manoil, C. General and condition-specific essential functions of *Pseudomonas aeruginosa*. *Proc. Natl. Acad. Sci. U. S. A.* **2015**, *112*, 5189–5194.
- (15) Valentino, M. D.; Foulston, L.; Sadaka, A.; Kos, V. N.; Villet, R. A.; Santa Maria, J., Jr.; Lazinski, D. W.; Camilli, A.; Walker, S.; Hooper, D. C.; Gilmore, M. S. Genes contributing to *Staphylococcus aureus* fitness in abscess- and infection-related ecologies. *mBio* **2014**, *5*, e01729–14.
- (16) Sasseti, C. M.; Boyd, D. H.; Rubin, E. J. Genes required for mycobacterial growth defined by high density mutagenesis. *Mol. Microbiol.* **2003**, *48*, 77–84.
- (17) Hedstrom, L. The bare essentials of antibiotic target validation. *ACS Infect. Dis.* **2017**, *3*, 2–4.
- (18) Petrelli, R.; Vita, P.; Torquati, I.; Felczak, K.; Wilson, D. J.; Franchetti, P.; Cappellacci, L. Novel inhibitors of inosine monophosphate dehydrogenase in patent literature of the last decade. *Recent Pat. Anti-Cancer Drug Discovery* **2013**, *8*, 103–125.
- (19) Makowska-Grzyska, M.; Kim, Y.; Wu, R.; Wilton, R.; Gollapalli, D. R.; Wang, X. K.; Zhang, R.; Jedrzejczak, R.; Mack, J. C.; Maltseva, N.; Mulligan, R.; Binkowski, T. A.; Gornicki, P.; Kuhn, M. L.; Anderson, W. F.; Hedstrom, L.; Joachimiak, A. Bacillus anthracis inosine 5'-monophosphate dehydrogenase in action: the first bacterial series of structures of phosphate ion-, substrate-, and product-bound complexes. *Biochemistry* **2012**, *51*, 6148–6163.
- (20) Usha, V.; Gurucha, S. S.; Lovering, A. L.; Lloyd, A. J.; Papaemmanouil, A.; Reynolds, R. C.; Besra, G. S. Identification of novel diphenyl urea inhibitors of Mt-GuaB2 active against. *Microbiology* **2011**, *157*, 290–299.
- (21) Makowska-Grzyska, M.; Kim, Y.; Gorla, S. K.; Wei, Y.; Mandapati, K.; Zhang, M.; Maltseva, N.; Modi, G.; Boshoff, H. I.; Gu, M.; Aldrich, C.; Cuny, G. D.; Hedstrom, L.; Joachimiak, A. *Mycobacterium tuberculosis* IMPDH in complexes with substrates, products and antitubercular compounds. *PLoS One* **2015**, *10*, No. e0138976.
- (22) Chen, L.; Wilson, D. J.; Xu, Y.; Aldrich, C. C.; Felczak, K.; Sham, Y. Y.; Pankiewicz, K. W. Triazole-linked inhibitors of inosine monophosphate dehydrogenase from human and. *J. Med. Chem.* **2010**, *53*, 4768–4778.
- (23) Usha, V.; Hobrath, J. V.; Gurucha, S. S.; Reynolds, R. C.; Besra, G. S. Identification of novel Mt-GuaB2 inhibitor series active against *M. tuberculosis*. *PLoS One* **2012**, *7*, No. e33886.
- (24) Park, Y.; Pacitto, A.; Bayliss, T.; Cleghorn, L. A.; Wang, Z.; Hartman, T.; Arora, K.; Ioerger, T. R.; Sacchetti, J.; Rizzi, M.; Donini, S.; Blundell, T. L.; Ascher, D. B.; Rhee, K. Y.; Breda, A.; Zhou, N.; Dartois, V.; Jonnal, S. R.; Via, L. E.; Mizrahi, V.; Epemolu, O.; Stojanovski, L.; Simeons, F. R.; Osuna-Cabello, M.; Ellis, L.; MacKenzie, C. J.; Smith, A. R.; Davis, S. H.; Murugesan, D.; Buchanan, K. I.; Turner, P. A.; Huggett, M.; Zuccotto, F.; Rebollo-Lopez, M. J.; Lafuente-Monasterio, M. J.; Sanz, O.; Santos Diaz, G.; Lelievre, J.; Ballell, L.; Selenski, C.; Axtman, M.; Ghidelli-Disse, S.; Pflaumer, H.; Boesche, M.; Drewes, G.; Freiberg, G.; Kurnick, M. D.; Srikumaran, M.; Kempf, D. J.; Green, S. R.; Ray, P. C.; Read, K. D.; Wyatt, P. G.; Barry Rd, C. E.; Boshoff, H. I. Essential but not vulnerable: indazole sulfonamides targeting inosine monophosphate dehydrogenase as potential leads against. *ACS Infect. Dis.* **2017**, *3*, 18–23.
- (25) Singh, V.; Donini, S.; Pacitto, A.; Sala, C.; Hartkoorn, R. C.; Dhar, N.; Keri, G.; Ascher, D. B.; Mondesert, G.; Vocat, A.; Lupien, A.; Sommer, R.; Vermet, H.; Lagrange, S.; Buechler, J.; Warner, D. F.; McKinney, J. D.; Pato, J.; Cole, S. T.; Blundell, T. L.; Rizzi, M.; Mizrahi, V. The inosine monophosphate dehydrogenase, GuaB2, is a vulnerable new bactericidal drug target for tuberculosis. *ACS Infect. Dis.* **2017**, *3*, 5–17.
- (26) Cox, J. A.; Mugumbate, G.; Del Peral, L. V.; Jankute, M.; Abrahams, K. A.; Jervis, P.; Jackenkroll, S.; Perez, A.; Alemparte, C.; Esquivias, J.; Lelievre, J.; Ramon, F.; Barros, D.; Ballell, L.; Besra, G. S. Novel inhibitors of *Mycobacterium tuberculosis* GuaB2 identified by a target based high-throughput phenotypic screen. *Sci. Rep.* **2016**, *6*, 38986.
- (27) Moffat, J. G.; Vincent, F.; Lee, J. A.; Eder, J.; Prunotto, M. Opportunities and challenges in phenotypic drug discovery: an industry perspective. *Nat. Rev. Drug Discovery* **2017**, *16*, 531–543.
- (28) Koul, A.; Arnoult, E.; Lounis, N.; Guillemont, J.; Andries, K. The challenge of new drug discovery for tuberculosis. *Nature* **2011**, *469*, 483–490.

- (29) Payne, D. J.; Gwynn, M. N.; Holmes, D. J.; Pompliano, D. L. Drugs for bad bugs: confronting the challenges of antibacterial discovery. *Nat. Rev. Drug Discovery* **2007**, *6*, 29–40.
- (30) Scott, D. E.; Coyne, A. G.; Hudson, S. A.; Abell, C. Fragment-based approaches in drug discovery and chemical biology. *Biochemistry* **2012**, *51*, 4990–5003.
- (31) Mendes, V.; Blundell, T. L. Targeting tuberculosis using structure-guided fragment-based drug design. *Drug Discovery Today* **2017**, *22*, 546–554.
- (32) Marchetti, C.; Chan, D. S.; Coyne, A. G.; Abell, C. Fragment-based approaches to TB drugs. *Parasitology* **2018**, *145*, 184–195.
- (33) Wei, Y.; Kuzmic, P.; Yu, R.; Modi, G.; Hedstrom, L. Inhibition of inosine-5'-monophosphate dehydrogenase from *Bacillus anthracis*: Mechanism revealed by pre-steady-state kinetics. *Biochemistry* **2016**, *55*, 5279–5288.
- (34) Dunkern, T.; Prabhu, A.; Kharkar, P. S.; Goebel, H.; Rolser, E.; Burckhard-Boer, W.; Arumugam, P.; Makhija, M. T. Virtual and experimental high-throughput screening (HTS) in search of novel inosine 5'-monophosphate dehydrogenase II (IMPDH II) inhibitors. *J. Comput.-Aided Mol. Des.* **2012**, *26*, 1277–1292.
- (35) Gorla, S. K.; Kavitha, M.; Zhang, M.; Chin, J. E.; Liu, X.; Striepen, B.; Makowska-Grzyska, M.; Kim, Y.; Joachimiak, A.; Hedstrom, L.; Cuny, G. D. Optimization of benzoxazole-based inhibitors of *Cryptosporidium parvum* inosine 5'-monophosphate dehydrogenase. *J. Med. Chem.* **2013**, *56*, 4028–4043.
- (36) Kitagawa, H.; Ozawa, T.; Takahata, S.; Iida, M.; Saito, J.; Yamada, M. Phenylimidazole derivatives of 4-pyridone as dual inhibitors of bacterial enoyl-acyl carrier protein reductases FabI and FabK. *J. Med. Chem.* **2007**, *50*, 4710–4720.
- (37) Soh, C. H.; Chui, W. K.; Lam, Y. An efficient and expeditious synthesis of di- and monosubstituted 2-aminoimidazoles. *J. Comb. Chem.* **2008**, *10*, 118–122.
- (38) Kumar, S.; Jaller, D.; Patel, B.; LaLonde, J. M.; DuHadaway, J. B.; Malachowski, W. P.; Prendergast, G. C.; Muller, A. J. Structure based development of phenylimidazole-derived inhibitors of indoleamine 2,3-dioxygenase. *J. Med. Chem.* **2008**, *51*, 4968–4977.
- (39) Jost, C.; Nitsche, C.; Scholz, T.; Roux, L.; Klein, C. D. Promiscuity and selectivity in covalent enzyme inhibition: a systematic study of electrophilic fragments. *J. Med. Chem.* **2014**, *57*, 7590–7599.
- (40) Fortin, S.; Moreau, E.; Lacroix, J.; Cote, M. F.; Petitclerc, E.; Gaudreault, R. C. Synthesis, antiproliferative activity evaluation and structure-activity relationships of novel aromatic urea and amide analogues of N-phenyl-N'-(2-chloroethyl)ureas. *Eur. J. Med. Chem.* **2010**, *45*, 2928–2937.
- (41) Bellina, F.; Guazzelli, N.; Lessi, M.; Manzini, C. Imidazole analogues of resveratrol: synthesis and cancer cell growth evaluation. *Tetrahedron* **2015**, *71*, 2298–2305.
- (42) Ascher, D. B.; Cromer, B. A.; Morton, C. J.; Volitakis, I.; Cherny, R. A.; Albiston, A. L.; Chai, S. Y.; Parker, M. W. Regulation of insulin-regulated membrane aminopeptidase activity by its C-terminal domain. *Biochemistry* **2011**, *50*, 2611–2622.
- (43) Kabsch, W. *Acta Crystallogr., Sect. D: Biol. Crystallogr.* **2010**, *66*, 125–132.
- (44) Adams, P. D.; Afonine, P. V.; Bunkoczi, G.; Chen, V. B.; Davis, I. W.; Echols, N.; Headd, J. J.; Hung, L. W.; Kapral, G. J.; Grosse-Kunstleve, R. W.; McCoy, A. J.; Moriarty, N. W.; Oeffner, R.; Read, R. J.; Richardson, D. C.; Richardson, J. S.; Terwilliger, T. C.; Zwart, P. H. PHENIX: a comprehensive Python-based system for macromolecular structure solution. *Acta Crystallogr., Sect. D: Biol. Crystallogr.* **2010**, *66*, 213–221.
- (45) Emsley, P.; Cowtan, K. Coot: model-building tools for molecular graphics. *Acta Crystallogr., Sect. D: Biol. Crystallogr.* **2004**, *60*, 2126–2132.
- (46) Jubb, H. C.; Higuieruelo, A. P.; Ochoa-Montano, B.; Pitt, W. R.; Ascher, D. B.; Blundell, T. L. Arpeggio: A web server for calculating and visualising interatomic interactions in protein structures. *J. Mol. Biol.* **2017**, *429*, 365–371.
- (47) Pires, D. E.; Blundell, T. L.; Ascher, D. B. mCSM-lig: quantifying the effects of mutations on protein-small molecule affinity in genetic disease and emergence of drug resistance. *Sci. Rep.* **2016**, *6*, 29575.
- (48) Pires, D. E.; Ascher, D. B. CSM-lig: a web server for assessing and comparing protein-small molecule affinities. *Nucleic Acids Res.* **2016**, *44*, W557–61.
- (49) Pires, D. E.; Blundell, T. L.; Ascher, D. B. pkCSM: Predicting small-molecule pharmacokinetic and toxicity properties using graph-based signatures. *J. Med. Chem.* **2015**, *58*, 4066–4072.
- (50) Singh, V.; Brecik, M.; Mukherjee, R.; Evans, J. C.; Svetlikova, Z.; Blasko, J.; Surade, S.; Blackburn, J.; Warner, D. F.; Mikusova, K.; Mizrahi, V. The complex mechanism of antimycobacterial action of 5-fluorouracil. *Chem. Biol.* **2015**, *22*, 63–75.